Article

Cell Metabolism

Control of Feeding Behavior by Cerebral Ventricular Volume Transmission of Melanin-Concentrating Hormone

Graphical Abstract

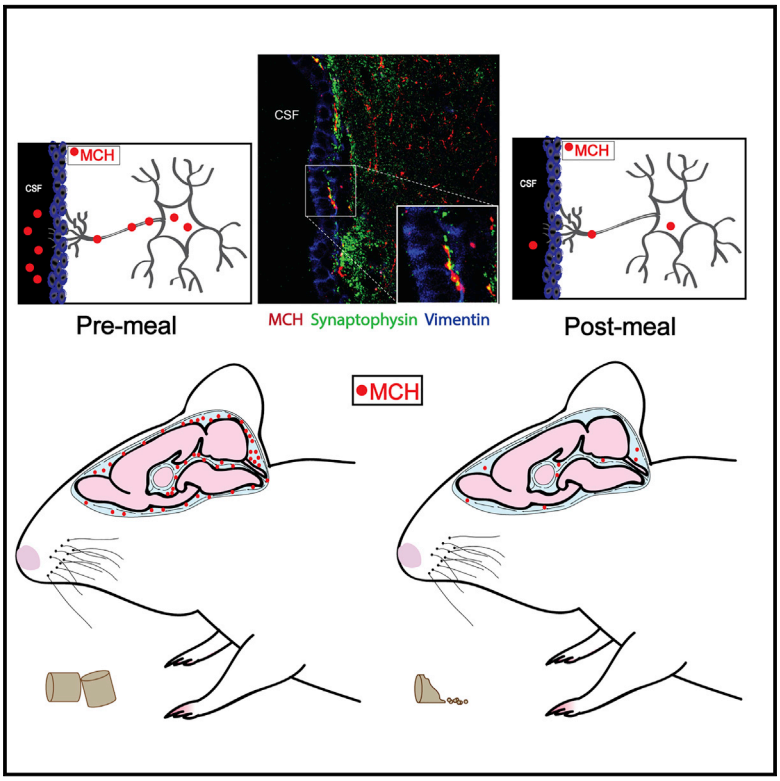

Highlights

- MCH neurons project to cerebral spinal fluid (CSF) in the brain ventricular system
- Chemogenetic activation of CSF-contacting MCH neurons increases food intake
- Reducing the bioavailability of endogenous MCH in the CSF inhibits food intake
- Humoral CSF neuropeptide transmission may be a common biological signaling pathway

Authors

Emily E. Noble, Joel D. Hahn, Vaibhav R. Konanur, ..., Martin Darvas, Suzanne M. Appleyard, Scott E. Kanoski

Correspondence

kanoski@usc.edu

In Brief

Noble et al. identify a biological signaling mechanism whereby the neuropeptide melanin-concentrating hormone is transmitted via the brain cerebrospinal fluid (CSF) to increase feeding behavior. These findings suggest that neuropeptide transmission through the CSF may be an important signaling mechanism through which the brain regulates fundamental behaviors.

Noble et al., 2018, Cell Metabolism *28*, 1–14
July 3, 2018
https://doi.org/10.1016/j.cmet.2018.05.001

CellPress

Please cite this article in press as: Noble et al., Control of Feeding Behavior by Cerebral Ventricular Volume Transmission of Melanin-Concentrating Hormone, Cell Metabolism (2018), https://doi.org/10.1016/j.cmet.2018.05.001

Cell Metabolism
Article

Control of Feeding Behavior by Cerebral Ventricular Volume Transmission of Melanin-Concentrating Hormone

Emily E. Noble,[1] Joel D. Hahn,[2] Vaibhav R. Konanur,[3] Ted M. Hsu,[1,4] Stephen J. Page,[5] Alyssa M. Cortella,[1] Clarissa M. Liu,[1,4] Monica Y. Song,[4] Andrea N. Suarez,[1] Caroline C. Szujewski,[1] Danielle Rider,[1] Jamie E. Clarke,[1] Martin Darvas,[6] Suzanne M. Appleyard,[5] and Scott E. Kanoski[1,4,7,*]

[1]Human and Evolutionary Biology Section, Department of Biological Sciences, University of Southern California, 3616 Trousdale Parkway, AHF-252, Los Angeles, CA 90089-0372, USA
[2]Neurobiology Section, Department of Biological Sciences, University of Southern California, Los Angeles, CA 90089, USA
[3]Neuroscience Graduate Program, University of Illinois, Chicago, IL 60612, USA
[4]Neuroscience Graduate Program, University of Southern California, Los Angeles, CA 90089, USA
[5]Program in Neuroscience, Department of Integrative Physiology and Neuroscience, Washington State University, Pullman, WA 99164, USA
[6]Department of Pathology, University of Washington, Seattle, WA 98195, USA
[7]Lead Contact
*Correspondence: kanoski@usc.edu
https://doi.org/10.1016/j.cmet.2018.05.001

SUMMARY

Classical mechanisms through which brain-derived molecules influence behavior include neuronal synaptic communication and neuroendocrine signaling. Here we provide evidence for an alternative neural communication mechanism that is relevant for food intake control involving cerebroventricular volume transmission of the neuropeptide melanin-concentrating hormone (MCH). Results reveal that the cerebral ventricles receive input from approximately one-third of MCH-producing neurons. Moreover, MCH cerebrospinal fluid (CSF) levels increase prior to nocturnal feeding and following chemogenetic activation of MCH-producing neurons. Utilizing a dual viral vector approach, additional results reveal that selective activation of putative CSF-projecting MCH neurons increases food intake. In contrast, food intake was reduced following immunosequestration of MCH endogenously present in CSF, indicating that neuropeptide transmission through the cerebral ventricles is a physiologically relevant signaling pathway for energy balance control. Collectively these results suggest that neural-CSF volume transmission signaling may be a common neurobiological mechanism for the control of fundamental behaviors.

INTRODUCTION

The brain regulates physiology and behavior, in part, through neuronal release of neuropeptides, neurotransmitters, and other small molecules. These signals act primarily through "wired" synaptic communication between neurons, between non-neuronal target cells and neurons, and through neuroendocrine signaling via the vasculature. A complementary neural communication pathway examined in the present study involves release and dispersal of brain-derived molecules through the cerebral spinal fluid (CSF) to reach distal targets, a neuroendocrine-like humoral mechanism termed "volume transmission" or "bulk flow" communication (Agnati et al., 1986). While brain-derived biological systems have previously been postulated to utilize a CSF volume transmission pathway to regulate fundamental behaviors such as stress, energy balance, and reproduction (Caraty and Skinner, 2008; Hoistad et al., 2005; Hsu et al., 2015a; MacMillan et al., 1998; Skinner and Malpaux, 1999; Veening et al., 2010), the physiological relevance of neuronal communication through CSF transmission has not yet been systemically investigated.

The present study examines whether melanin-concentrating hormone (MCH), a neuropeptide produced primarily by neurons in the lateral hypothalamic area (LHA) and zona incerta (ZI) that increases appetite and food intake (Barson et al., 2013; Bittencourt et al., 1992; Qu et al., 1996; Shimada et al., 1998), exerts its stimulatory effects on feeding via release into CSF and volume transmission through the brain. Through the melanin-concentrating hormone receptor 1 (MCH 1R), MCH both increases food intake and reduces energy expenditure, promoting overall elevated weight gain in rodents (Chambers et al., 1999; Kowalski et al., 2004; Lembo et al., 1999; Shearman et al., 2003). The importance of this neuropeptide system to overall energy balance is highlighted by findings showing that rodents lacking MCH (Shimada et al., 1998) or MCH 1R (Marsh et al., 2002) are lean, whereas transgenic MCH overexpression produces hyperphagia and obesity (Ludwig et al., 2001). While the central distribution of MCH 1R is extensive and spans throughout the brain neuraxis (Chee et al., 2013; Lembo et al., 1999), the sites of action and neurobiological mechanisms through which MCH stimulates feeding are poorly understood.

We hypothesized that MCH regulates feeding, in part, by neural-CSF volume transmission, and tested this hypothesis utilizing

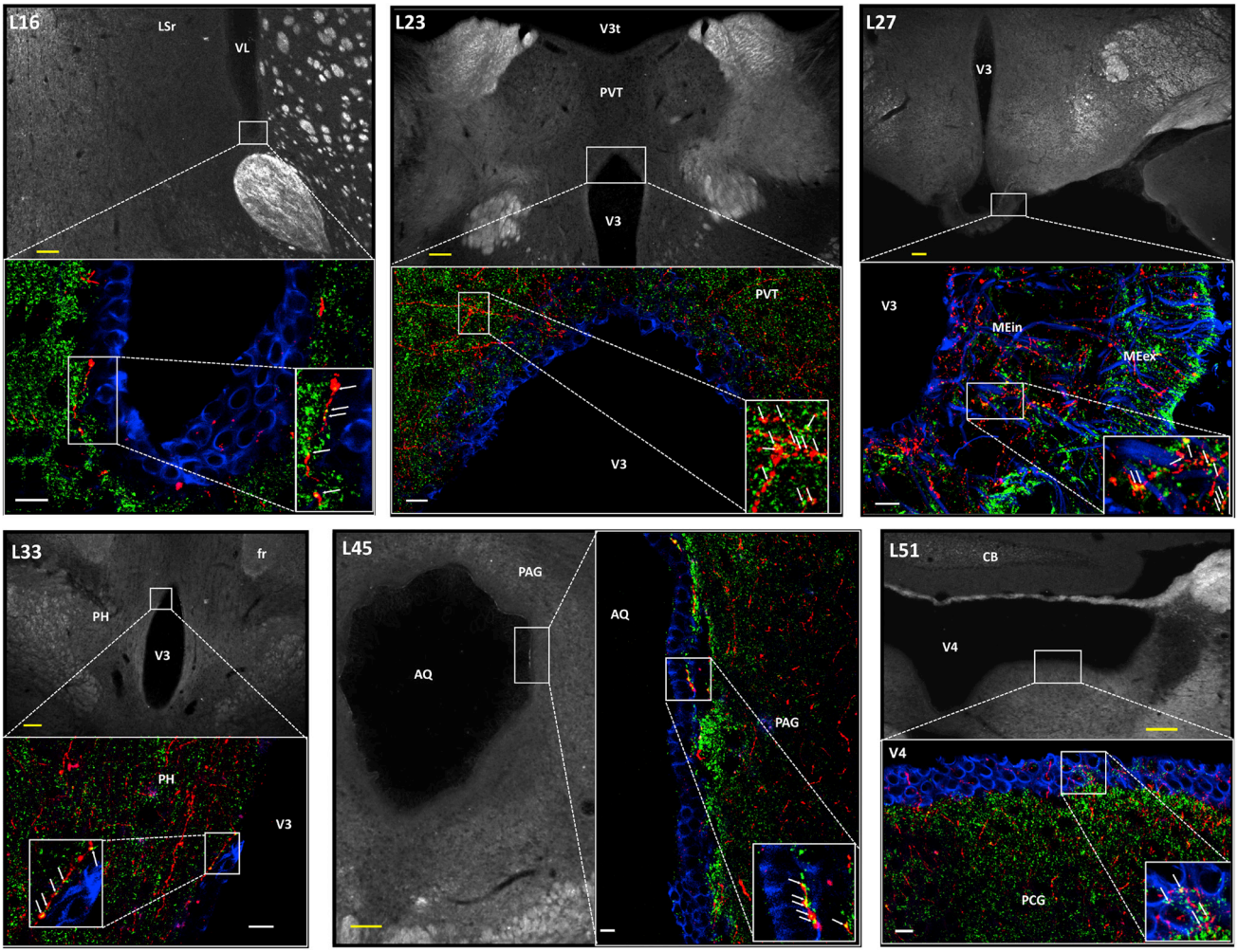

Figure 1. MCH-Producing Neurons Terminate in the Ependymal Layer Lining the Cerebral Ventricles

Immunofluorescence co-labeling of MCH and synaptophysin at the ventricular ependymal layer supports the possibility of cerebroventricular volume transmission. Red, MCH axons; green, synaptophysin (synaptic vesicle marker); blue, vimentin (ventricular ependymal cell marker). Arrows indicate MCH+ synaptophysin co-labeling. Numbers in the upper left in each image preceded by L indicate correspondence to closest atlas levels of the rat brain atlas of Swanson (Swanson, 2004). aco, anterior commissure; AQ, cerebral aqueduct; CB, cerebellum; fr, fasciculus retroflexus; LSr, lateral septal nucleus, rostral part; MEex, median eminence; MEin, median eminence, internal lamina; PAG, periaqueductal gray; PCG, pontine central gray; PH, posterior hypothalamic nucleus; PVH, paraventricular hypothalamic nucleus; PVT, paraventricular thalamic nucleus; V3, third ventricle; V3t, third ventricle, thalamic part; V4, fourth ventricle; VL, lateral ventricle. Scale bars, 10 μm (white) and 100 μm (yellow).

multiple levels of analysis in the rat. Collectively, our findings identify a population of MCH neurons that communicate with the CSF and we further reveal that MCH present in the CSF is functionally relevant to feeding behavior. These results implicate humoral volume transmission of brain-derived molecules through the cerebral ventricles as a physiological signaling pathway relevant to the control of fundamental behaviors.

RESULTS

The Cerebral Ventricles Receive Direct Input from MCH Neurons

We conducted a series of neuroanatomical investigations to establish a basis for possible CSF transmission of MCH. Tri-label immunofluorescence was performed for MCH, vimentin (a marker of cerebral ventricle-lining ependymal cells), and synaptophysin (a marker of synaptic vesicles). Confocal microscopic analysis revealed the presence of synaptophysin-immunoreactive (ir) elements co-localized with MCH-ir axon terminals in close apposition to vimentin-ir ependymal cells lining the cerebral aqueduct and the lateral, third, and fourth ventricles (Figure 1). These results support the possibility of release of MCH into the CSF from MCH-producing neurons.

To determine the extent and distribution of MCH-expressing neurons involved in putative MCH-CSF signaling, a complimentary set of experiments combined immunofluorescence detection of MCH with retrograde neural pathway tracing. Intracerebroventricular (i.c.v.) injections of cholera toxin B (CTB) (a retrograde tracer that enters cells from axon terminals) combined with immunofluorescent labeling for MCH-expressing

cell bodies revealed co-localization of CTB and MCH-ir labeling in approximately one-third (32.7%) of MCH-ir somata within the LHA and ZI; this represented 43.8% of CTB-labeled somata in the LHA and ZI. Furthermore, high spatial resolution analysis revealed a wide range of regional differences in the levels of co-localization (Figures 2A and 2B). These data, combined with the tri-label immunofluorescence data, establish a structural basis for putative neural-CSF MCH transmission, and suggest that it is highly organized and extensive.

Based on the presence of MCH-ir terminals in the median eminence (Figure 1), a hypothalamic region where neuroendocrine cells interface with the vasculature, we sought to determine the extent to which CSF-signaling MCH neurons might also be neuroendocrine cells. To investigate this, we combined intravenous injections of fast blue (FB) (a retrograde pathway tracer) with i.c.v. injections of CTB and immunofluorescence detection of MCH. Established neuroendocrine regions contained FB, including the paraventricular nucleus of the hypothalamus (PVH) (Figure S1) and supraoptic nucleus (not shown). Analyses of the co-localization of CTB with FB in MCH neurons indicated that only very few MCH neurons are neuroendocrine (0.4%), and similarly very few CTB-containing MCH neurons (i.e., putative CSF-contacting MCH neurons) also project to the vasculature (~1.2%) (Figure 2C). In addition, PVH neuroendocrine neurons do not express MCH and only rarely collateralize to CSF (indicated by rare occurrences of FB and CTB or MCH co-labeling) (Figure S1). Taken together the data indicate that a substantial subset of MCH neurons project to CSF, almost all of which do not communicate via neuroendocrine pathways.

To determine whether other feeding-relevant neuropeptide systems are anatomically conducive to CSF-mediated ventricular transmission, comparable neuroanatomical analyses were conducted for the neuropeptide hypocretin/orexin (H/O). H/O was selected as a viable candidate because H/O-expressing neurons are intermingled with MCH neurons in the LHA, yet form a distinct population (Hahn, 2010; Swanson et al., 2005). Moreover, like MCH, H/O is implicated in control of feeding and energy balance and also (unlike MCH) promotes arousal, activity, and energy expenditure (for review see Barson et al., 2013; Kotz et al., 2006). Analyses revealed abundant H/O and CTB co-labeling in the LHA (Figure 3A), accounting for 42% of LHA CTB-ir neurons retrogradely labeled following i.c.v. CTB injections. Additional tri-label immunofluorescence and confocal microscopic analysis for H/O, synaptophysin, and vimentin indicated the presence of H/O terminals in close apposition to ependymal cells lining the lateral, third, and fourth cerebral ventricles (Figure 3B). These findings indicate that, like MCH, H/O neurons contact CSF extensively and throughout the neuraxis.

Since a portion of MCH neurons are known to co-express the inhibitory neurotransmitter GABA (Harthoorn et al., 2005), we further characterized the CSF-contacting MCH neurons to reveal whether this population of cells is neurochemically distinct from other MCH neurons with regard to GAD67-ir (a GABAergic marker). Analyses indicated that 45% of CTB-labeled MCH-ir neurons were GAD67-ir, compared with 23.5% of MCH-ir neurons that do not contact CSF (Figure 4A). These data suggest that CSF-signaling MCH neurons are more likely to be GABAergic compared with MCH neurons that do not communicate to the CSF. Furthermore, using a combined approach of fluorescence *in situ* hybridization with immunohistochemical staining we detected no measurable mRNA expression levels of the glutamatergic marker VGlut2 in CTB-positive MCH-ir neurons (Figure 4B), nor were CTB-positive MCH-ir neurons co-localized with VGlut1 or VGlut3 mRNA-expressing neurons (not shown). These findings suggest that CSF-signaling MCH neurons are likely not glutamatergic. Given that a large percent of CSF-contacting MCH neurons are GABAergic, and that ventricular injections of both the GABA-A (Kokare et al., 2006) and GABA-B (Ebenezer, 1990) receptor agonists increase food intake, we reasoned it possible that MCH and GABA may act synergistically in the CSF to promote feeding. However, this is unlikely as we found that neither the GABA-A receptor agonist muscimol (Figures 4C and 4D) nor the GABA-B receptor agonist baclofen (Figure 4E) potentiated a feeding response when injected i.c.v. in combination with a sub-effective dose of MCH. Thus, while none of the CSF-contacting MCH neurons are glutamatergic and almost half are GABAergic, GABA co-release does not appear to be critical for MCH feeding effects.

CSF MCH Levels Are Increased Following MCH Neuron Activation and Prior to Feeding

To determine if MCH levels in CSF are elevated following selective MCH neuron activation, rats were bilaterally injected in the LHA and ZI with an adeno-associated virus (AAV) containing an excitatory designer receptor exclusively activated by designer drugs (DREADDs) driven by an MCH-specific promoter, and containing the mCherry reporter (AAV2-rMCHp-hM3D(Gq)-mCherry). Immunofluorescence co-localization of MCH-ir and mCherry confirmed selective infection of MCH neurons with the DREADDs, as no mCherry-ir cell bodies were observed that were not also MCH-ir (Figure 5A). To confirm that hM3D(Gq) receptors are physiologically functional in MCH neurons, slice electrophysiological recordings from LHA mCherry-positive DREADDs receptor-containing MCH neurons show that application of the DREADDs receptor ligand, clozapine-N-oxide (CNO), increases the firing rate of infected cells (Figures 5B–5D). To confirm that hM3D(Gq) receptors are functional in MCH neurons at the behavioral level, i.c.v. injections of CNO in rats that were bilaterally infected with the AAV2-rMCHp-hM3D(Gq)-mCherry significantly elevated food intake, an effect that was blocked by pretreatment with i.c.v. injections of the MCH 1R antagonist H6408 (Figure 5E). While this experiment was performed during the dark cycle when animals normally eat, we also observed that animals infected with MCH DREADDs had elevated food intake when CNO injections were given prior to feeding during the light cycle (data not shown). Together these data show that hM3D(Gq) receptors are functional in MCH neurons, and that chemogenetic activation of an indiscriminate population of MCH-producing neurons increases feeding via an MCH 1R-mediated mechanism. Moreover, these results support those from the previous experiment in suggesting that GABA co-release is not functionally relevant for MCH feeding effects, as the hyperphagic effects of chemogenetic MCH neuron activation were completely blocked with i.c.v. co-delivery of an MCH 1R antagonist.

We next reasoned that, if MCH is transmitted through CSF to increase feeding behavior, then activation of MCH neurons should elevate MCH levels in CSF (Figure 6A). Following *in vivo*

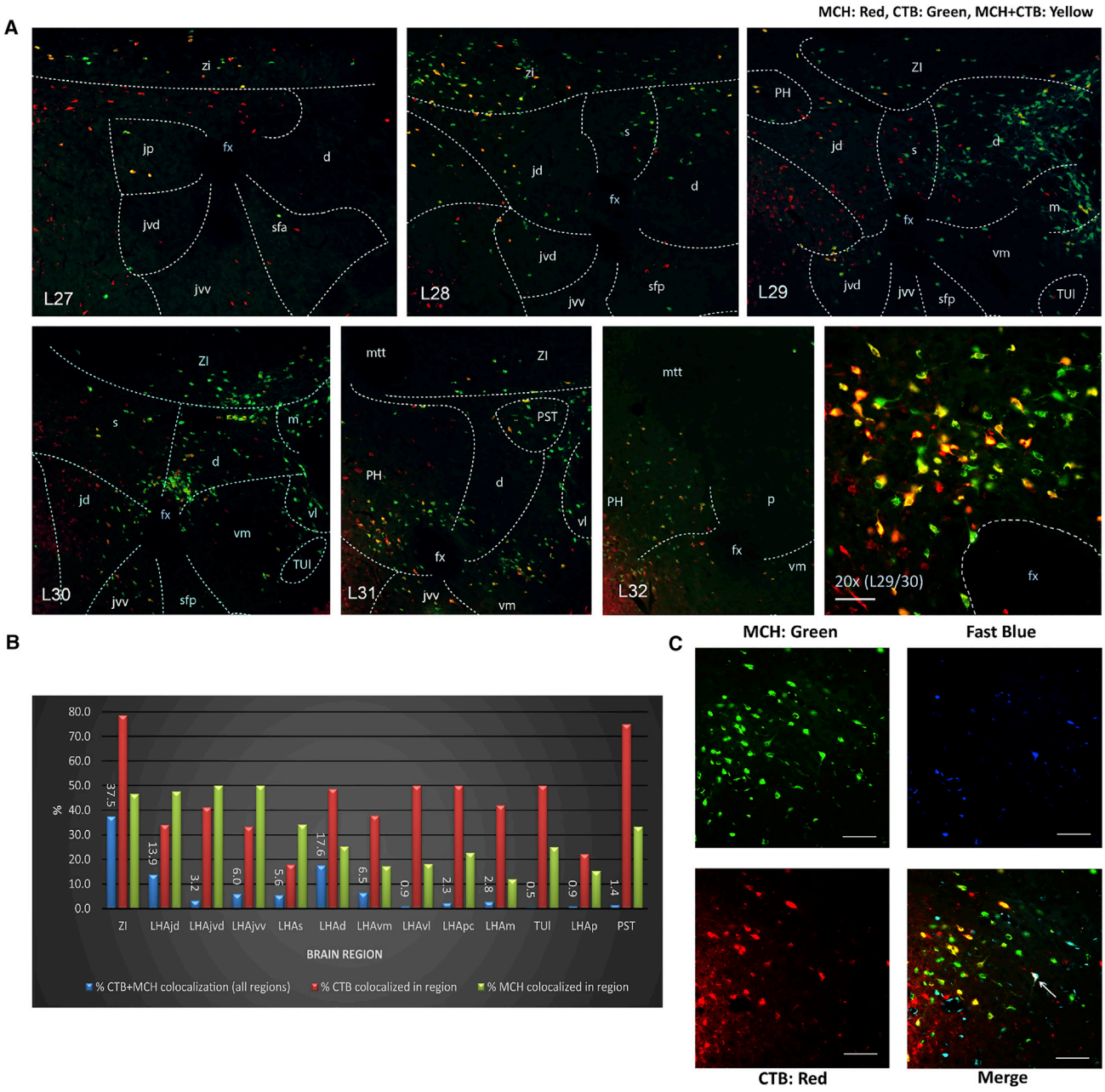

Figure 2. Approximately One-Third of All MCH Neurons Are CSF Projecting, and these Neurons Are Distinct from Neuroendocrine Neurons

(A) Distribution of MCH immunolabeled and CTB retrogradely labeled neurons following lateral ventricular CTB injections; representative immunofluorescence for MCH (green), CTB (red), and co-labeled cells (yellow). Numbers in the lower left in each image preceded by L indicate correspondence to closest atlas levels of the rat brain atlas of Swanson (Swanson, 2004).

(B) Overall, 32.7% of MCH-ir somata within the LHA and ZI were also CTB-ir, whereas 43.8% of CTB-ir somata in the LHA and ZI were MCH-ir. Percentages of co-labeling for the ZI and for specific LHA sub-regions are represented as follows: blue bars indicate the percentage of total (across all brain regions) co-localized MCH-ir + CTB-ir located in each region; red bars indicate the percentage CTB-ir neurons that are co-localized with MCH-ir in each region; green bars indicate the percentage MCH-ir neurons that are co-localized with CTB-ir in each region.

(C) Representative images of immunofluorescence for MCH (green), CTB (red), and fast blue (FB) (blue) in the LHA. Intravenously injected FB retrogradely labeled neurons with access to the vasculature (putative neuroendocrine neurons). Overall 98.8% of MCH + CTB analyzed were not labeled with FB, with the arrow pointing to an extremely rare instance of a triple-labeled cell (MCH + CTB + FB). d, LHA dorsal region; fx, fornix; jd, LHA juxtadorsomedial region; jp, LHA juxtaparaventricular region; jvd, LHA juxtaventromedial region, dorsal zone; jvv, LHA juxtaventromedial region, ventral zone; m, LHA magnocellular nucleus; mtt, mammillothalamic tract; p, LHA posterior region; pc, LHA parvicellular region; PH, posterior hypothalamic nucleus; PST, preparasubthalamic nucleus; s, LHA suprafornical region; sfa, LHA subfornical region, anterior zone; sfp, LHA subfornical region, posterior zone; TUI, tuberal nucleus, lateral part; vl, LHA ventral region, lateral zone; vm, LHA medial zone, ventral region; ZI, zona incerta. Scale bars, 50 μm.

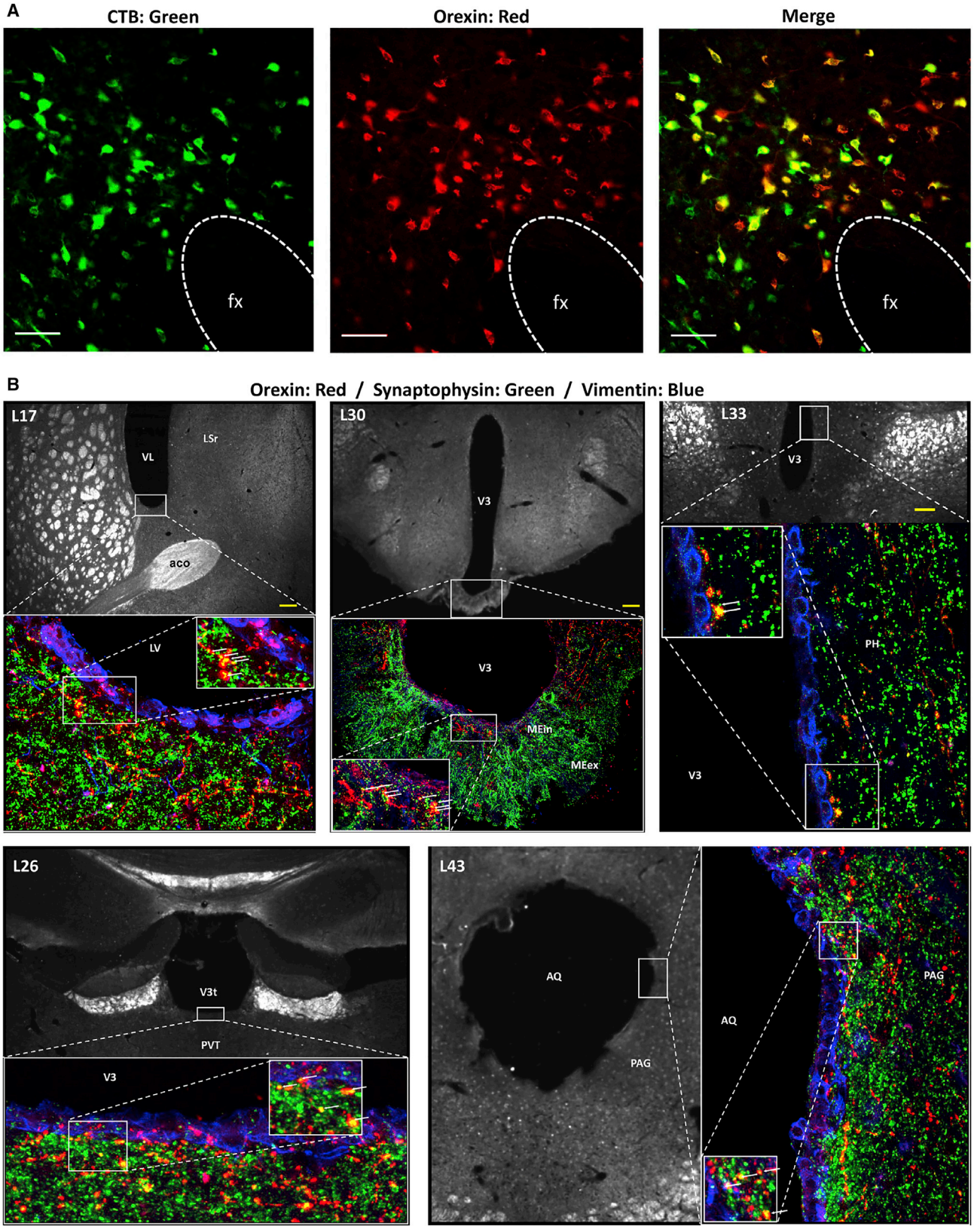

(legend on next page)

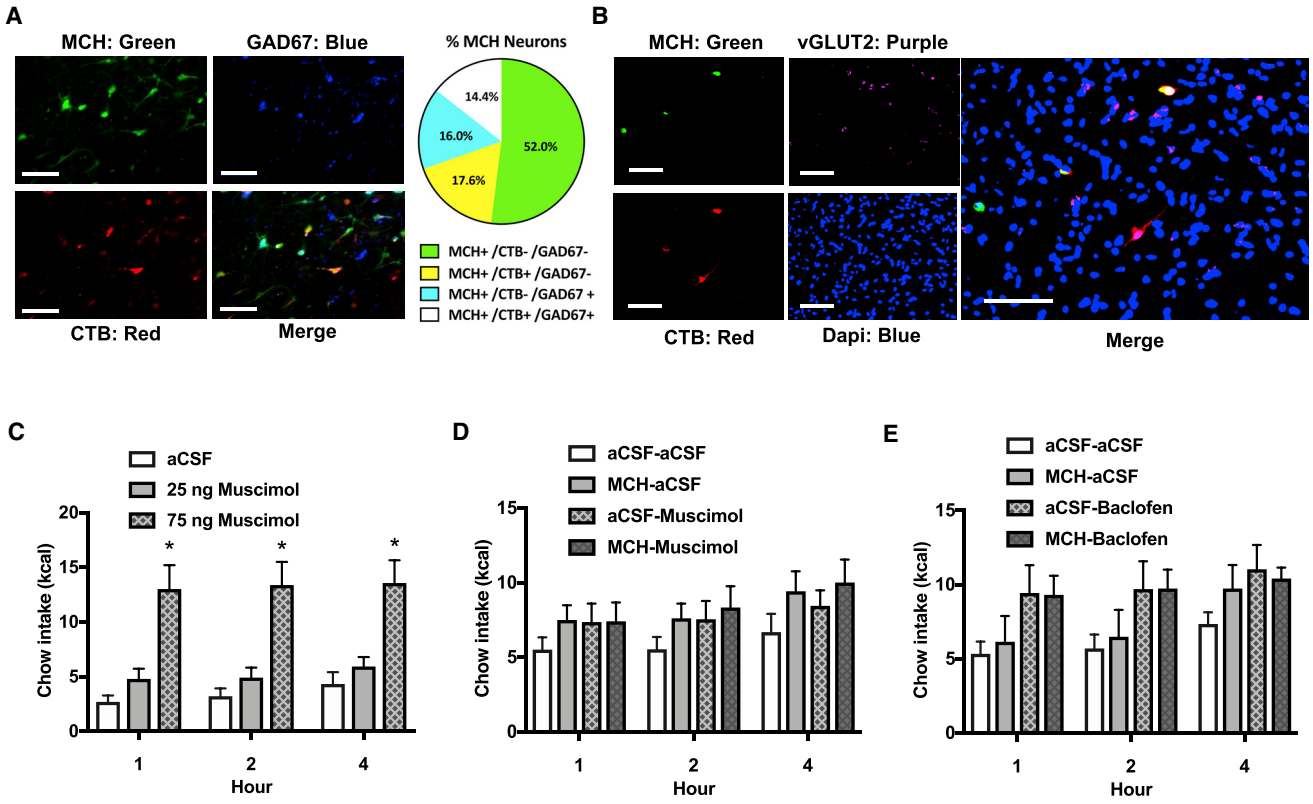

Figure 4. While 45% of CSF-Projecting MCH Neurons Co-express GABAergic Markers, GABA Signaling Is Unlikely to Interact with MCH-Driven Hyperphagia

(A) CTB was injected into the lateral ventricle and immunofluorescent staining was performed for MCH (green), CTB (red), and the GABAergic marker GAD67 (blue). Quantification indicated that 14.4% of MCH neurons were both GABAergic (GAD67 immunolabeled) and CSF signaling (CTB retrogradely labeled following CTB injection into the lateral ventricle), whereas 17.6% of CTB-positive MCH neurons did not contain the GABAergic marker. Thus 45% of putative CSF-signaling MCH neurons were GABAergic, compared with 23.5% of MCH neurons that are putative non-CSF signaling. Scale bars, 50 μm.

(B) CTB was injected into the lateral ventricle and immunofluorescent staining was performed for MCH (red) and CTB (green), followed by fluorescence *in situ* hybridization for the glutamatergic marker VGlut2 (purple). Quantification indicated that there was no co-localization of VGlut2 in CTB-positive MCH-ir neurons, nor was there co-localization of VGlut1 or VGlut3 (data not shown). Scale bars, 100 μm.

(C) A dose response for the effects of i.c.v. injections of the GABA-A receptor agonist muscimol indicated a significant effect of drug where 75 ng significantly elevated food intake while 25 ng was ineffective (n = 12) (*p<.0001).

(D) i.c.v. injection of a sub-effective dose of muscimol (20 ng) did not potentiate the feeding effects of a sub-effective dose of MCH (0.5 μg) (n = 12).

(E) i.c.v. injection of a sub-effective dose of baclofen (0.1 nmol) did not potentiate the feeding effects of a sub-effective dose of MCH (0.5 μg) (n = 19).

extraction of CSF from the cisterna magna of the rat (~200–250 μL/rat, approximating the entire CSF pool from an adult rat) (Figure 6B), MCH protein quantification detected via enzyme immunosorbent assay revealed the presence of MCH in CSF under physiological conditions. Moreover, following chemogenetic activation of the MCH neurons (by i.c.v. CNO injections first delivered at 120 min and a second injection 15 min prior to extracting CSF) and subsequent processing of the CSF as described above, animals had significantly higher CSF MCH levels compared with vehicle treatment. These results show that selective activation of MCH neurons increases MCH release into the CSF and thereby corroborate neuroanatomical data indicating that MCH neurons release MCH into the CSF (Figure 6C).

To determine whether the concentrations of CSF MCH achieved after chemogenetic MCH neuron activation were comparable with those achieved following i.c.v. pharmacological injection of a feeding-relevant dose of MCH, we first determined that 1 μg is the lowest effective dose of i.c.v. MCH to significantly

Figure 3. Approximately 40% of Hypocretin/Orexin-Producing Neurons Project to CSF

(A) Representative images of CTB (red), hypocretin/orexin (H/O) (green), and co-labeled neurons (yellow) in the LHA. The presence of CTB retrograde labeling in H/O-ir neurons after CTB injection into the lateral ventricle indicates that some H/O neurons project to the CSF. fx, fornix. Scale bars, 50 μm.

(B) Immunofluorescence co-labeling of H/O and synaptophysin at the cerebroventricular ependyma supports the possibility of volume transmission into the CSF. Synaptophysin (a synaptic vesicle marker) and H/O co-labeling was present at the site of ependymal cells immunolabeled for vimentin (a marker of ependymal cells) at multiple locations within the cerebral ventricles. Red, H/O axons; green, synaptophysin; blue, vimentin. Arrows indicate H/O + synaptophysin co-labeling. Numbers upper left in each image preceded by L indicate correspondence to closest atlas levels of the rat brain atlas of Swanson (Swanson, 2004).

aco, anterior commissure; AQ, cerebral aqueduct; LSr, lateral septal nucleus, rostral part; VL, lateral ventricle; ME, median eminence; PAG, periaqueductal gray; PH, posterior hypothalamic nucleus; PVH, hypothalamic paraventricular nucleus; PVT, paraventricular thalamic nucleus; V3, third ventricle. Scale bars, 100 μm.

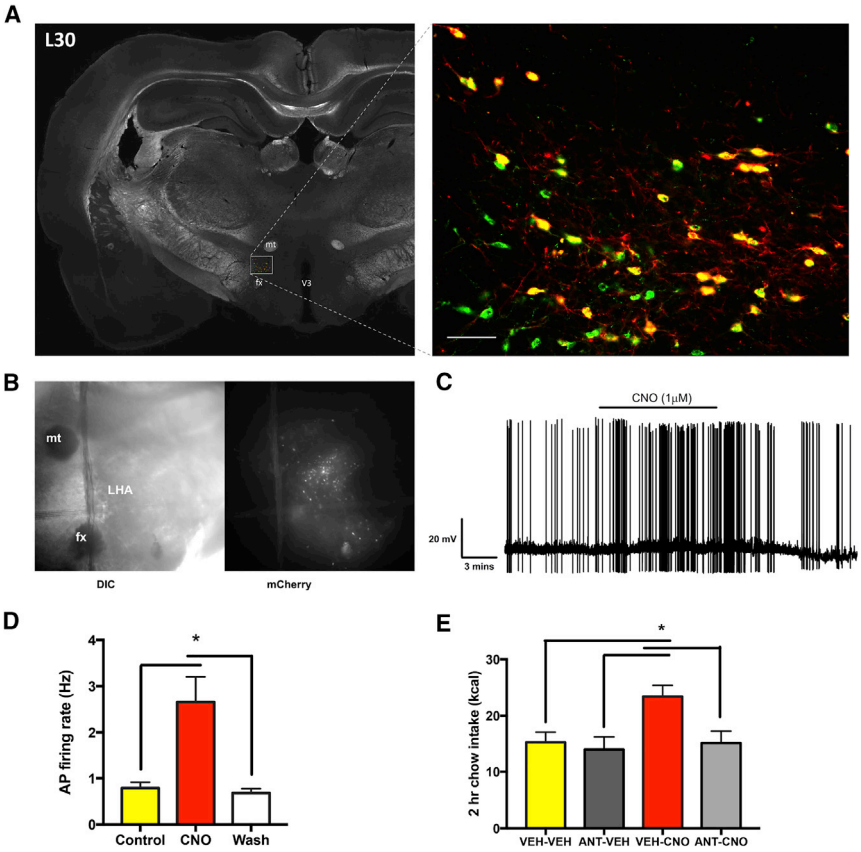

Figure 5. Viral Transduction of Designer Receptors Exclusively Activated by Designer Drugs (hM3Gq) Is a Valid Method of Inducing Selective and Functionally Relevant Activation of MCH Neurons

(A) Representative images of the mCherry reporter gene present in MCH neurons, indicating successful infection of the designer receptors exclusively activated by designer drugs (DREADDs) adeno-associated virus (AAV) selective in MCH neurons. MCH, green; mCherry, red; co-localization, yellow. Scale bar, 50 μm.

(B) Representative differential interference contrast (DIC) and fluorescence microscopy images of hypothalamic slice preparations.

(C) Representative trace of electrophysiological recordings from mCherry-positive DREADDs-expressing MCH neurons before, during, and after clozapine-N-oxide (CNO) (the DREADDs ligand) application.

(D) Rats were bilaterally injected in the LHA and ZI with an AAV driving hM3Gq DREADDs expression under the control of a promoter for MCH (AAV2-rMCHp-hM3D(Gq)-mCherry). Data from electrophysiological recordings showing that CNO significantly increased the firing rate of mCherry-positive DREADDs-expressing MCH neurons ($n = 8$) (*$p < 0.005$).

(E) CNO (18 mmol) was used to pharmacologically activate MCH neurons, which resulted in increased feeding that was blocked by pretreatment with the MCH 1R antagonist H6408 (ANT) (10 μg) ($n = 7,8$/group) (*$p < 0.05$).

All data are represented as means ± SEM. mt, mammillothalamic tract; fx, fornix; V3, third ventricle.

increase food intake (Figure S2A). Next, we found that i.c.v. injections of this dose of MCH raised MCH CSF levels to similar levels as MCH DREADDs activation (166.4 ± 24.13 and 136.5 ± 31.45 pg/mL, respectively) (Figure S2B). These findings indicate that, compared with what would be predicted mathematically, pharmacologically effective doses of i.c.v. MCH raise CSF MCH levels by relatively small incremental amounts. This outcome is not surprising, and is likely due to interactions with unidentified neurophysiological mechanisms that prolong MCH peptide integrity and/or enhance MCH ligand-receptor binding affinity under physiological conditions.

We next investigated whether MCH CSF levels are physiologically altered by feeding-relevant parameters. CSF MCH levels were measured during the inactive phase when rodents are not normally eating (light cycle), during the early dark cycle just prior to consumption of the first meal after light offset (typically one of the largest meals in a rodent's feeding cycle [Johnson et al., 1986] [dark pre]), during the dark cycle following ingestion of a standardized meal of 5 g of chow (dark post), and during the late dark cycle in *ad libitum*-fed animals that were food restricted for only 1 hr prior to CSF extraction (dark, late, fed). Results reveal that CSF MCH levels were elevated pre-prandially during the dark cycle compared with the postprandial state (dark post), late in the dark cycle (dark, late, fed), and compared with the inactive cycle (light cycle). These findings support the hypothesis that endogenous CSF MCH signaling plays a role in stimulating feeding at the beginning of the active dark cycle, when rodents normally consume their biggest meal (Figure 6D).

Several experiments were then conducted to determine whether MCH CSF levels are dynamically regulated by meal entrainment, maintenance diet, and/or acute food restriction. Relative to levels during the light cycle in *ad libitum*-fed rats, MCH CSF levels were not different at the onset of a conditioned food access period in rats that were previously meal entrained to consume all of their daily chow within a 4-hr period during the light cycle (Figure 6E). This suggests that CSF MCH levels are not easily entrainable by scheduled light-cycle feeding (food intake and body weight data depicted in Figures S3A–S3C). Moreover, consumption of a palatable high-fat diet (HFD) for 2 weeks did not elevate pre-prandial levels of CSF MCH during the dark cycle compared with animals fed *ad libitum* chow (Figure 6F), despite the elevated caloric intake and weight gain of animals fed an HFD (Figures S3D and S3E). Further, we did not observe elevations in MCH levels late during the dark cycle in *ad libitum*-fed animals compared with animals that were 48-hr food deprived (Figure 6G), despite significantly reduced body weights at the time of CSF extraction (Figure S3F). Taken together these data reveal that CSF MCH levels are not dynamically regulated by meal entrainment, maintenance diet, or acute food deprivation. Rather, the data suggest that MCH CSF release is under circadian control with a putative function of promoting the initial feeding bout during the nocturnal feeding cycle.

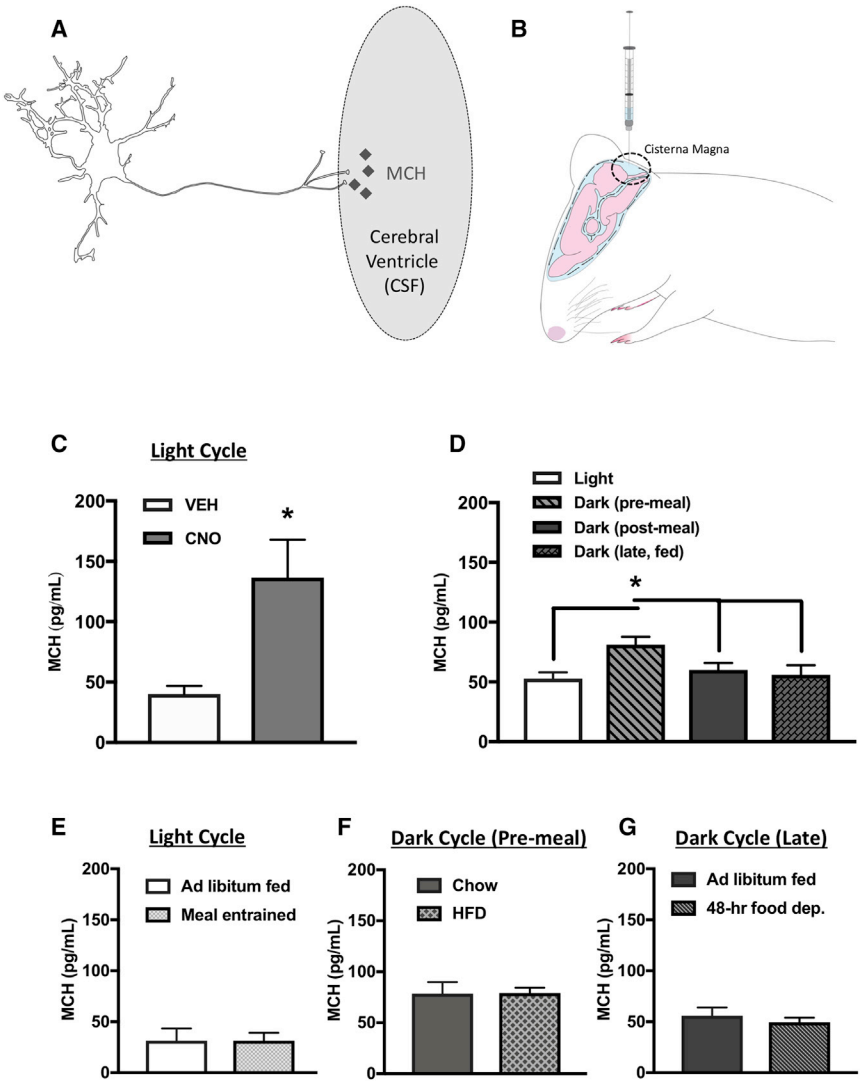

Figure 6. MCH Levels in the CSF Are Increased by DREADDs-Mediated Activation of MCH Neurons and Prior to Nocturnal Feeding

(A) A hypothetical model whereby MCH is transmitted into the CSF through axon terminals of ventricular-contacting terminals from MCH neurons.

(B) Cartoon demonstrating the method of CSF extraction from the cisterna magna of an anesthetized rat.

(C) MCH levels were elevated in CSF following MCH DREADDs activation (n = 6 and 7) (*p = 0.02).

(D) Under physiological conditions, MCH levels in CSF are elevated during the early dark cycle prior to food consumption compared with during the light cycle and dark cycle postprandially (n = 6–8) (*$p < 0.05$).

(E) There were no differences in CSF MCH levels prior to light-cycle feeding in meal entrained animals compared with *ad libitum*-fed controls (n = 7/group).

(F) Five days of exposure to a palatable high-fat diet had no effect on pre-prandial CSF MCH levels during the early dark cycle compared with chow-fed animals (n = 6/group).

(G) Forty-eight hours of food deprivation had no effect on CSF MCH levels during the late dark cycle compared with *ad libitum*-chow-fed controls (n = 5 and 6/group). Data are mean ± SEM.

This is consistent with previous literature revealing that MCH mRNA expression peaks at the beginning of the dark cycle (Bluet-Pajot et al., 1995).

Activation of CSF-Contacting MCH Neurons Increases Food Intake

To directly examine the contribution of the CSF-signaling MCH neurons to feeding behavior, we utilized a dual-virus approach to selectively activate the population of MCH neurons that project to CSF. The retrograde-transported canine adenovirus type 2 containing the genetic information for cre recombinase (CAV2-CRE) (Boender et al., 2014) was injected into the lateral ventricle and a cre-dependent MCH DREADDs AAV type 2 (AAV2-DIO-MCH DREADDs-hM3D(Gq)-mCherry) was injected into the LHA and ZI (Figure 7A). This dual-virus approach targets the expression of the hM3D(Gq) DREADDs receptor only to the subset of MCH neurons that have axon terminals contacting the CSF. The selectivity of DREADDs expression in CSF-contacting MCH neurons was corroborated by co-localization of mCherry, MCH, and CTB following i.c.v. injections of CTB (Figure 7B). Quantification of mCherry-positive cells revealed that this dual-virus approach infected ~8% of the number of cells infected using the non-cre-dependent DREADs virus. Subsequent i.c.v. CNO injections in these animals revealed that selective activation of CSF-projecting MCH neurons significantly elevated food intake (Figure 7C), indicating that chemogenetic-mediated activation of CSF-signaling MCH neurons is sufficient to produce a hyperphagic response.

From these data, we cannot exclude the possibility that the elevated food intake response was based, in part, on activation of collateral synaptic projections from MCH neurons that make contact with CSF. One region where parenchymal pharmacological injections of MCH have been shown to elevate feeding is the nucleus accumbens shell (ACBsh) (Georgescu et al., 2005). To determine whether MCH neurons that project to the CSF have collateral projections to the ACBsh, we first injected the retrograde tracer Fluoro-Gold into the ACBsh, and the retrograde tracer CTB into the lateral ventricle, and performed immunofluorescent labeling for MCH. Results indicated that an extremely small percentage (~0.08%) of MCH neurons that project to the CSF have collateral projections to the ACBsh (Figures S4A and S4B).

Next, we examined whether DREADDs-mediated activation of ACBsh-projecting MCH neurons increases food intake. The retrograde-transported CAV2-CRE was injected into bilaterally into the ACBsh and a cre-dependent MCH DREADDs AAV type 2 (AAV2-DIO-MCH DREADDs-hM3D(Gq)-mCherry) was

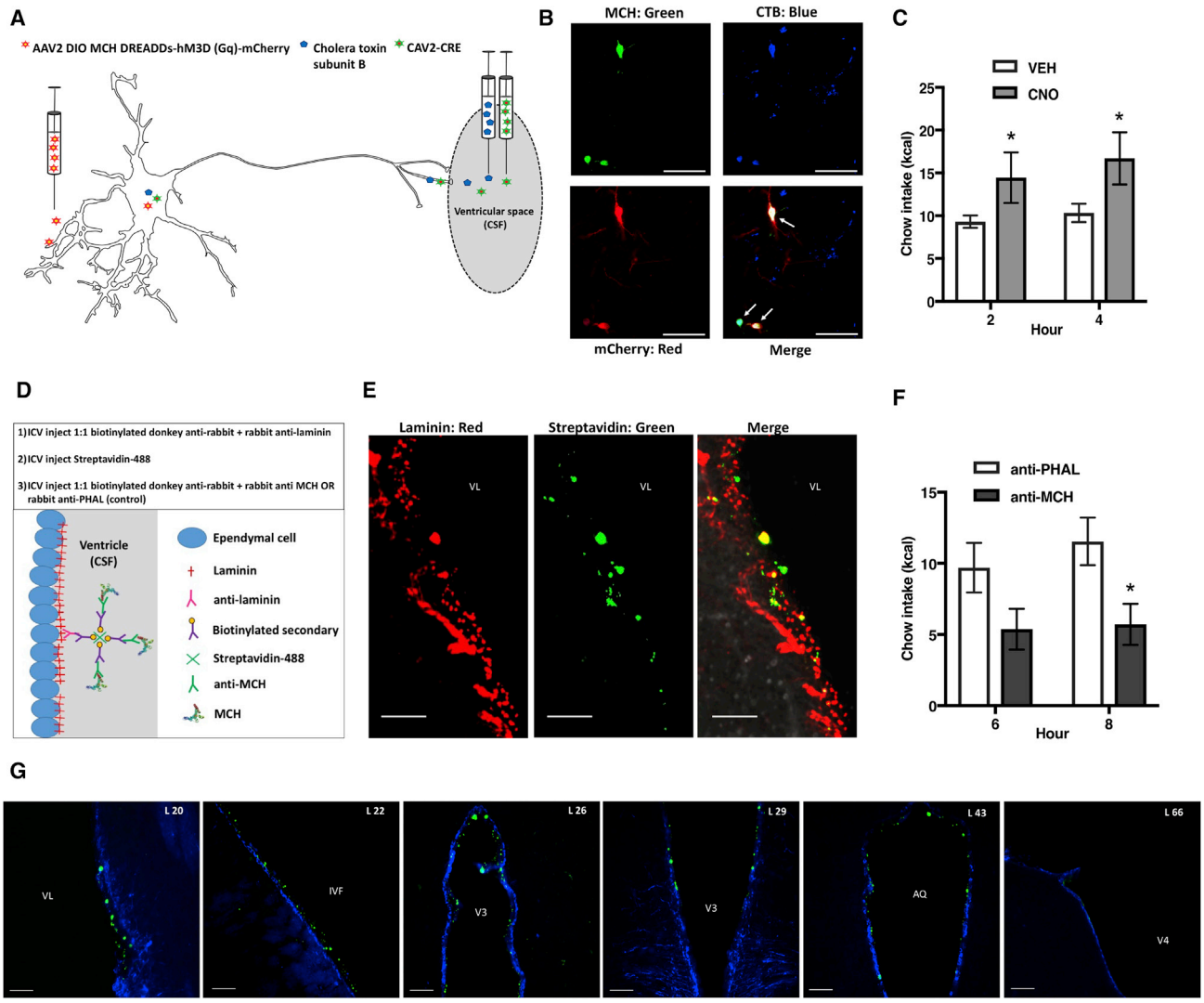

Figure 7. Selective Activation of Ventricular-Projecting MCH Neurons Increases Feeding, Whereas Feeding Is Reduced by Immunosequestration of MCH Endogenously Present in the CSF

(A) To selectively activate ventricular projecting MCH neurons, we utilized a dual-virus strategy (1) the retrograde canine adenovirus type 2 containing cre recombinase (CAV2-CRE) was injected into the lateral ventricle, and (2) a cre-dependent MCH DREADDs AAV serotype 2 (AAV2-DIO-MCH DREADDs-hM3D(Gq)-mCherry) was injected into the LHA and ZI.

(B) Epifluorescence image showing mCherry labeling (red) co-localized with MCH immunolabeling (green), and cells retrogradely labeled by the retrograde tracer CTB (blue), following lateral ventricle CTB injection. Arrows indicate triple colocalization of CTB, mCherry, and MCH immunolabeling.

(C) Activation of ventricular projecting MCH neurons by lateral ventricular injections of CNO increases food intake (n = 7) (*$p < 0.05$).

(D) A cartoon depicting the strategy and steps of an immunosequesteration approach designed to reduce the bioavailability of endogenous CSF MCH.

(E) A representative image showing immunofluorescence labeling of laminin (red), streptavidin-Alexa Fluor 488 (green), and their co-localization (yellow) at the ventricular ependymal layer (indicating that anti-MCH immunoglobulins were localized with laminin-ir at the ventricular ependyma).

(F) Results from the immuno-sequestration experiment indicated that under normal physiological conditions a reduction in the bioavailability of CSF MCH significantly reduces food intake (n = 8 and 9) (*$p < 0.05$).

(G) Representative immunofluorescence images showing the rostral-caudal spread of streptavidin-Alexa Fluor 488 (green) localized at the ventricular ependyma (shown with vimentin immunofluorescence in blue), indicating extensive rostral caudal CSF MCH immunosequestration. The numbers in the upper left in each image preceded by L indicate correspondence to closest atlas levels of the rat brain atlas of Swanson (Swanson, 2004) (*$p < 0.05$).

Data are means ± SEM. Scale bars, 50 μm in (B and E) and 100 μm in (G). AL, atlas level; AQ, cerebral aqueduct; IVF, intraventricular foramen; V3, third ventricle; V4, fourth ventricle; VL, lateral ventricle.

injected into the LHA and ZI. Quantification of one of five series from each injected animal revealed that an average of ~9% of cells infected with the non-cre-dependent DREADDs were infected using the dual-virus approach with CAV2-CRE targeting the ACBsh, which is comparable with the percentage infected using intraventricular injections of CAV2-CRE (~8%). More detailed anatomical analyses revealed differences in the location of cell populations containing the mCherry reporter, with the

highest expression of ACBsh-projecting MCH DREADDs transduced neurons in the ZI (atlas level 28) and the highest expression of i.c.v.-projecting MCH DREADDs transduced neurons in the LHAd at atlas level 30 (based on the Swanson Atlas [Swanson, 2004] [Figure S5]). Our behavioral results show that the same dose of i.c.v. CNO that was effective for increasing food intake when DREADDs were targeted to CSF-contacting MCH neurons (Figure 7C; 18 mmol) had no effect on food intake when DREADDs were targeted to ACB-projecting MCH neurons (Figure S4C). Importantly, that i.c.v. CNO injections did not affect food intake when DREADDs were targeted to ACBsh-projecting MCH neurons indicates that the hyperphagic effects of i.c.v. CNO injections in rats with DREADDs targeted to CSF-projecting MCH neurons are not based on back-transformation of CNO into the non-inert molecule clozapine (and non-specific clozapine binding), an outcome that has been demonstrated following peripheral injections of a high dose (5 mg/kg) of CNO injections in rats (MacLaren et al., 2016). Collectively, these results indicate that the elevated food intake following activation of CSF-contacting MCH neurons is not based on collateral projections to the ACBsh, nor is it based on non-specific clozapine binding.

Blockade of MCH Endogenously Present in the CSF Reduces Food Intake

To determine the endogenous relevance of MCH that is present CSF under physiological conditions to feeding behavior, we first injected animals with a neutralizing antibody against MCH or a non-endogenous molecule (control group; using primary antibodies directed against the lectin *Phaseolus vulgaris leucoagglutinin* (PHAL), and raised in the same species as the MCH primary), targeting the lateral ventricle. Injections were given just prior to the onset of the dark cycle, when animals normally consume their biggest meal. Using this approach, we found that food intake was significantly reduced in animals who received the MCH antibody injections compared with those in the control group (Figure S6A).

Postmortem tissue analyses using fluorescent secondary antibody-based immunofluorescence staining revealed that some of the antibody likely diffused into the neuropil (Figure S6B, "neutralizing antibody approach"), which means that the reduction in food intake could potentially be based on neutralization of MCH present in the neuropil surrounding the ventricles in addition to the CSF. Thus, we developed a three-step "immunosequestration" approach to selectively reduce the bioavailability of MCH present in the CSF while minimizing neuropil diffusion of antibody-protein complexes. The approach is as follows: (1) a primary antibody directed against the extracellular matrix protein laminin (expressed in ependymal cells lining the cerebral ventricles) was mixed with a biotinylated secondary antibody directed against the species of the primary antibody; this complex was then injected into the lateral ventricle. This first step was designed to anchor biotin molecules to laminin-expressing ependymal cells lining the cerebral ventricles. (2) Fluorescently labeled streptavidin, which contains four binding sites for biotin, was injected into the lateral ventricle. This second step was designed to exploit the high binding affinity of biotin and avidin, resulting in fluorescently labeled avidin molecules anchored to the cerebral ventricle walls. (3) Injections were given into the lateral ventricle of another primary/biotinylated secondary antibody complex, with the primary antibody directed against either MCH (experimental group) or a non-endogenous molecule (PHAL; control group). The aim of this third step was to enable the binding of conjugated biotin in the complex to free streptavidin binding sites on the ependymal cells lining the ventricles (Figure 7D). This approach was designed to sequester endogenous MCH in the CSF to the ependymal ventricle/neuropil junction, reducing its bioavailability and preventing transport of MCH in the CSF into the neuropil. In contrast with the neutralizing antibody approach, we did not observe a haze surrounding the ventricular region at the injection site following our postmortem immunofluorescence analyses, indicating that it is less likely that antibodies diffused into the neuropil using our immunosequesteration approach (Figure S6B). The fluorescent streptavidin was visualized along the ventricular lining, indicating successful anchoring of the complex to the walls of the ventricle and not into the neuropil (Figure 7E). Injections were given just prior to the beginning of the active phase, when animals normally eat and when endogenous CSF MCH levels are elevated (e.g., Figure 6D). Food intake was significantly reduced in animals subjected to CSF MCH immunosequestration compared with those who received the PHAL control complex (Figure 7F). Rostral/caudal anatomical analyses through the ventricular system revealed that streptavidin was present throughout the forebrain and midbrain, but was minimally present in the caudal hindbrain 30 min after the third i.c.v. injection (Figure 7G). Similar anatomical distribution was observed 8 hr post injection (data not shown). These data show that the i.c.v. immunosequestration approach is effective for rapid and neuroanatomically extensive sequestration of antibody-protein complexes along the ventricular ependymal layer, and, importantly, corroborate the hypothesis that CSF transmission of MCH is physiologically relevant for feeding behavior.

DISCUSSION

Conceptually, volume transmission of brain-derived molecules (i.e., the transmission of signaling molecules through non-synaptic modalities) was explicitly proposed in 1986 by Agnati et al. as a complement to "wiring transmission" (i.e., the synaptic transmission between neurons, and between neurons and non-neuronal target cells that are in direct contact) (Agnati et al., 1986). In contrast to synaptic transmission, where communication is discrete and dependent on neuroanatomical connections, CSF transmission of neuropeptides and small-molecule neurotransmitters represents a neuroendocrine-like method of humoral transmission with the potential for widespread neuromodulation of distal regions of the brain (Veening and Barendregt, 2010). Indeed recent findings show that unidentified neuromodulators are present in human CSF in sufficient quantities to excite neurons, thereby supporting the plausibility of CSF transmission as a mechanism for system-wide modulation of neuronal activity (Bjorefeldt et al., 2015). However, the physiological contribution of CSF transmission to regulating behavior has remained hypothetical and largely understudied, possibly due in part to the technical challenge of separating the effects CSF-mediated signaling from concurrent synaptic transmission. Here we apply multiple levels of analysis to confirm the feasibility of endogenous CSF transmission of MCH, and further confirm that this pathway is a major contributor to the control of feeding behavior.

Prior findings revealed that MCH gene expression peaks during the early stages of the dark cycle, supporting a potential role for circadian fluctuations in driving MCH expression and subsequent peptide release (Bluet-Pajot et al., 1995). Consistent with this, we observed that endogenous CSF MCH levels are highest pre-prandially at the onset of the dark cycle compared with (1) postprandially following a fixed meal in the early nocturnal phase, (2) late in the dark cycle after *ad libitum* feeding, and (3) during the inactive light cycle. These findings suggest a framework in which a circadian mechanism stimulates an increase in CSF MCH release at the beginning of the feeding/nocturnal cycle with the putative goal of driving the first feeding bout of the active phase. Consistent with this model, our additional data suggest that endogenous CSF MCH signaling may not be driving food intake due to various other factors, including acute food restriction, palatable obesogenic diet maintenance, and light-cycle meal entrainment.

Our data raise several important questions. Foremost, what are the sites of action through which CSF transmission of MCH (and other neuromodulators) elevates feeding? One consideration to take into account is the flow of CSF, which is rostral to caudal through the ventricular system and then proceeds through the cisternal subarachnoid space (Reiber, 2003). We observed immunoreactive terminals for MCH throughout the rostral-caudal extent of the ventricular system, suggesting that CSF MCH has widespread distribution throughout the neuraxis—a possibility that is consistent with the widespread central distribution of the MCH 1R (Lembo et al., 1999).

Our data also raise the question of in what form is MCH is released into the CSF. The CSF contains endopeptidases such as endopeptidase 24.11 and aminopeptidase M, which are known to degrade MCH (Maulon-Feraille et al., 2002; Muraki et al., 1996). It is possible that MCH is released in CSF in a form that protects it against rapid proteolytic degradation. For example, the pro-hormone peptide form of MCH (NEI-MCH) has been shown to be resistant to proteolytic degradation (Maulon-Feraille et al., 2002). This is one possible mechanism to explain why a 1-μg dose of exogenous MCH was required to elevate CSF MCH levels by only ~80 pg/mL (Figure S2). Alternatively, it is possible that MCH is released in the CSF in extracellular vesicles (exosomes). Indeed, exosomes that transport peptides have been identified in human CSF (Street et al., 2012). Future studies are necessary to identify the form in which MCH is transmitted in the CSF, as well as the downstream neural sites of action.

The extent to which MCH translocates from the CSF to the neuropil remains to be determined. Intercellular junctions between ependymal cells regulate the degree to which CSF contacts the extracellular fluid of the neuropil, and region-specific differences in these junctions exists (Vigh et al., 2004). One possibility is that MCH translocates into the neuropil through tanycytes, which are specialized ependymal cells lining the base of the lateral and third cerebral ventricles. For example, radiolabeled nerve growth factor injected into the CSF has been shown to translocate from the CSF through tanycytes and accumulate in the locus coeruleus (Feng et al., 2011). Moreover, the anorectic adipokine, leptin, is trafficked from the median eminence to mediobasal hypothalamic neurons via tanycyte-mediated transport into CSF (Balland et al., 2014). An additional possibility is that CSF MCH is able to alter feeding via activation of MCH 1R on cilia. Two types of cilia exist (primary and motile); interestingly, both types of cilia contain MCH 1R (Conductier et al., 2013; Hamamoto et al., 2016) and optogenetic-mediated activation of MCH neurons alters the tonic control of the ependymal motile cilia beat frequency and the CSF flow rate in mice (Conductier et al., 2013). It is unknown to what extent this function of MCH on motile cilia contributes to the feeding effects of CSF-transmitted MCH observed in the present study.

It is possible that CSF volume transmission through the cerebral ventricles is a commonly used means of biological communication for other brain-derived neuropeptides and small-molecule neurotransmitters. We investigated this possibility at the neuroanatomical level for the neuropeptide H/O, which, like MCH, is produced in the LHA in an intermingled yet distinct population of neurons (Hahn, 2010). As was observed for MCH, we identified H/O immunoreactive terminals at the site of ependymal cells lining multiple cerebral ventricular locations. Furthermore, ~40% of H/O neurons were labeled following injection of the retrograde pathway tracer, CTB, into the lateral ventricle, suggesting that both H/O- and MCH-producing neurons are transmitted through the CSF. Common to MCH and H/O systems is the engagement of G protein-coupled receptors to modulate core functions such as stress, energy balance, reproduction, glucose homeostasis, and sleep (Barson et al., 2013). It would be interesting for future studies to determine the relevance of CSF transmission of both H/O and MCH to each of these behaviors. A putative role for CSF H/O and MCH signaling in mediating sleep pathologies is suggested by findings that low levels of orexin A (hypocretin 1) were reported in the CSF of narcoleptic patients (Ripley et al., 2001), and that CSF MCH levels were altered by paradoxical sleep deprivation in rodents (Dias Abdo Agamme et al., 2015). Future studies are needed to determine whether CSF MCH extends to the control of sleep and other non-feeding behaviors, such as novelty detection, which was recently linked with MCH neuronal activity (Gonzalez et al., 2016). In addition to MCH and H/O, several different neuropeptide systems have been postulated to utilize a CSF volume transmission pathway, such as oxytocin (Veening et al., 2010), beta-endorphin (Hoistad et al., 2005; MacMillan et al., 1998), melatonin (Skinner and Malpaux, 1999), gonadotropin-releasing hormone (Caraty and Skinner, 2008), glucagon-like pepotide-1 (GLP-1) (Hsu et al., 2015a), and others. For example, intrastriatal injections of beta-endorphin can be detected in cerebrospinal fluid, suggesting that beta-endorphin may migrate out of the neuropil and be transmitted in CSF (Hoistad et al., 2005). Corroborating the likelihood of extrasynaptic beta-endorphin transmission (either via CSF or through interstitial volume transmission) is the presence of beta-endorphin immunoreactivity in the cerebral cortex (a region lacking beta-endorphin immunoreactive terminals) 60–90 min after stimulation of hypothalamic neurons (MacMillan et al., 1998). A similar receptor-terminal mismatch scenario was previously reported by our group for GLP-1 where we hypothesized that GLP-1 produced in hindbrain neurons reaches the hippocampus through CSF transmission (Hsu et al., 2015a). Future work is needed to determine whether these and other neuropeptide/neurotransmitter systems utilize CSF transmission to mediate behavior and behavioral state changes. Such examination will fundamentally advance understanding of

how various brain-derived molecules communicate to regulate physiology and behavior.

The possibility that behavioral and physiological state changes can be evoked by neuropeptidergic transmission in the CSF presents new avenues for clinical investigation. Lumbar spinal tap CSF sampling is commonly used to determine biomarkers for neurological disease such as Alzheimer's disease and related pathologies (Sheline et al., 2014), a practice based on the predominant zeitgeist of thought that the CSF is primarily a medium for flushing metabolic waste and other solutes from the brain's cellular tissue. However, the notion that the CSF is an active biological signaling medium opens up new possibilities for clinical insight derived from human CSF sampling. For example, CSF neuropeptide profiling may represent a biological thumbprint for susceptibility to future pathologies as opposed to simply indicating the presence of existing pathologies. In addition, novel therapies may be developed that target neural-CSF signaling pathways for the prevention or treatment of conditions such as metabolic syndrome, narcolepsy, and disorders of reproduction.

Limitations of the Study

While we observed a significant reduction in feeding using an antibody-based immunosequestration approach designed to reduce the bioavailability of MCH endogenously present in the CSF, a limitation of the study is that we were unable to accurately quantify the magnitude of the reduction of bioavailable MCH in CSF due to methodological limitations inherent in using an antibody-based approach. In addition, despite the use of immunohistochemistry amplification of fluorescent reporters, we cannot be certain regarding the percentage of cells that project to a given region (CSF or ACB) that were successfully targeted/transduced, and thus our quantification likely underestimated the total number of transduced cells that project to the respective regions. These limitations should be taken into account when interpreting our results.

STAR★METHODS

Detailed methods are provided in the online version of this paper and include the following:

SUPPLEMENTAL INFORMATION

Supplemental Information includes six figures and can be found with this article online at https://doi.org/10.1016/j.cmet.2018.05.001.

ACKNOWLEDGMENTS

The research was supported by DK104897 and institutional funds to S.E.K., institutional funds to M.D., DK083452 and institutional funds to S.M.A. (CVM, WSU), DK107333 to T.M.H., and DK111158 to E.E.N. The authors thank Dr. Alan Watts, Dr. Ruth Wood, Brian Zingg, Sandhya Prathap, Kaitlin Sontag, Natalie Demirjian, Emily Nakamoto, April Banayan, Victor Lee, and Dr. Matthew Dean for their conceptual and experimental contributions.

AUTHOR CONTRIBUTIONS

E.E.N., J.D.H., and S.E.K. designed the experiments and conceived the neural pathway tracing, chemogenetic, and immunosequestration strategies. Neuroanatomical experiments and analysis were performed by E.E.N., J.D.H., V.R.K., A.M.C., C.M.L., M.Y.S., A.N.S., C.C.S., D.R., J.E.C., and S.E.K. Behavioral experiments and analysis were performed by E.E.N., T.M.H., A.N.S., and C.M.L. Electrophysiology experiments and analysis were performed by S.J.P., E.E.N., and S.M.A. CAV2-CRE viral plasmids were prepared by M.D. The paper was written by E.E.N and S.E.K., with substantial editorial input from J.D.H. and additional editorial input from the other authors.

DECLARATION OF INTERESTS

The authors have no competing interests to declare.

Received: August 11, 2017
Revised: February 28, 2018
Accepted: May 2, 2018
Published: May 31, 2018

REFERENCES

Agnati, L.F., Fuxe, K., Zoli, M., Ozini, I., Toffano, G., and Ferraguti, F. (1986). A correlation analysis of the regional distribution of central enkephalin and beta-endorphin immunoreactive terminals and of opiate receptors in adult and old male rats. Evidence for the existence of two main types of communication in the central nervous system: the volume transmission and the wiring transmission. Acta Physiol. Scand. *128*, 201–207.

Balland, E., Dam, J., Langlet, F., Caron, E., Steculorum, S., Messina, A., Rasika, S., Falluel-Morel, A., Anouar, Y., Dehouck, B., et al. (2014). Hypothalamic tanycytes are an ERK-gated conduit for leptin into the brain. Cell Metab. *19*, 293–301.

Barson, J.R., Morganstern, I., and Leibowitz, S.F. (2013). Complementary roles of orexin and melanin-concentrating hormone in feeding behavior. Int. J. Endocrinol. *2013*, 983964.

Bittencourt, J.C., Presse, F., Arias, C., Peto, C., Vaughan, J., Nahon, J.L., Vale, W., and Sawchenko, P.E. (1992). The melanin-concentrating hormone system

of the rat brain: an immuno- and hybridization histochemical characterization. J. Comp. Neurol. *319*, 218–245.

Bjorefeldt, A., Andreasson, U., Daborg, J., Riebe, I., Wasling, P., Zetterberg, H., and Hanse, E. (2015). Human cerebrospinal fluid increases the excitability of pyramidal neurons in the in vitro brain slice. J. Physiol. *593*, 231–243.

Bluet-Pajot, M.T., Presse, F., Voko, Z., Hoeger, C., Mounier, F., Epelbaum, J., and Nahon, J.L. (1995). Neuropeptide-E-I antagonizes the action of melanin-concentrating hormone on stress-induced release of adrenocorticotropin in the rat. J. Neuroendocrinol. *7*, 297–303.

Boender, A.J., de Jong, J.W., Boekhoudt, L., Luijendijk, M.C., van der Plasse, G., and Adan, R.A. (2014). Combined use of the canine adenovirus-2 and DREADD-technology to activate specific neural pathways in vivo. PLoS One *9*, e95392.

Caraty, A., and Skinner, D.C. (2008). Gonadotropin-releasing hormone in third ventricular cerebrospinal fluid: endogenous distribution and exogenous uptake. Endocrinology *149*, 5227–5234.

Chambers, J., Ames, R.S., Bergsma, D., Muir, A., Fitzgerald, L.R., Hervieu, G., Dytko, G.M., Foley, J.J., Martin, J., Liu, W.S., et al. (1999). Melanin-concentrating hormone is the cognate ligand for the orphan G-protein-coupled receptor SLC-1. Nature *400*, 261–265.

Chee, M.J., Pissios, P., and Maratos-Flier, E. (2013). Neurochemical characterization of neurons expressing melanin-concentrating hormone receptor 1 in the mouse hypothalamus. J. Comp. Neurol. *521*, 2208–2234.

Conductier, G., Martin, A.O., Risold, P.Y., Jego, S., Lavoie, R., Lafont, C., Mollard, P., Adamantidis, A., and Nahon, J.L. (2013). Control of ventricular ciliary beating by the melanin concentrating hormone-expressing neurons of the lateral hypothalamus: a functional imaging survey. Front. Endocrinol. (Lausanne) *4*, 182.

Dias Abdo Agamme, A.L., Aguilar Calegare, B.F., Fernandes, L., Costa, A., Lagos, P., Torterolo, P., and D'Almeida, V. (2015). MCH levels in the CSF, brain preproMCH and MCHR1 gene expression during paradoxical sleep deprivation, sleep rebound and chronic sleep restriction. Peptides *74*, 9–15.

Ebenezer, I.S. (1990). The effect of intracerebroventricular administration of baclofen on food intake in rats. Neuroreport *1*, 73–76.

Feng, C.Y., Wiggins, L.M., and von Bartheld, C.S. (2011). The locus ceruleus responds to signaling molecules obtained from the CSF by transfer through tanycytes. J. Neurosci. *31*, 9147–9158.

Georgescu, D., Sears, R.M., Hommel, J.D., Barrot, M., Bolanos, C.A., Marsh, D.J., Bednarek, M.A., Bibb, J.A., Maratos-Flier, E., Nestler, E.J., et al. (2005). The hypothalamic neuropeptide melanin-concentrating hormone acts in the nucleus accumbens to modulate feeding behavior and forced-swim performance. J. Neurosci. *25*, 2933–2940.

Gonzalez, J.A., Iordanidou, P., Strom, M., Adamantidis, A., and Burdakov, D. (2016). Awake dynamics and brain-wide direct inputs of hypothalamic MCH and orexin networks. Nat. Commun. *7*, 11395.

Hahn, J.D. (2010). Comparison of melanin-concentrating hormone and hypocretin/orexin peptide expression patterns in a current parceling scheme of the lateral hypothalamic zone. Neurosci. Lett. *468*, 12–17.

Hamamoto, A., Yamato, S., Katoh, Y., Nakayama, K., Yoshimura, K., Takeda, S., Kobayashi, Y., and Saito, Y. (2016). Modulation of primary cilia length by melanin-concentrating hormone receptor 1. Cell. Signal. *28*, 572–584.

Harthoorn, L.F., Sane, A., Nethe, M., and Van Heerikhuize, J.J. (2005). Multitranscriptional profiling of melanin-concentrating hormone and orexin-containing neurons. Cell. Mol. Neurobiol. *25*, 1209–1223.

Hoistad, M., Samskog, J., Jacobsen, K.X., Olsson, A., Hansson, H.A., Brodin, E., and Fuxe, K. (2005). Detection of beta-endorphin in the cerebrospinal fluid after intrastriatal microinjection into the rat brain. Brain Res. *1041*, 167–180.

Hsu, T.M., Hahn, J.D., Konanur, V.R., Lam, A., and Kanoski, S.E. (2015a). Hippocampal GLP-1 receptors influence food intake, meal size, and effort-based responding for food through volume transmission. Neuropsychopharmacology *40*, 327–337.

Hsu, T.M., Hahn, J.D., Konanur, V.R., Noble, E.E., Suarez, A.N., Thai, J., Nakamoto, E.M., and Kanoski, S.E. (2015b). Hippocampus ghrelin signaling mediates appetite through lateral hypothalamic orexin pathways. Elife *4*, https://doi.org/10.7554/eLife.11190.

Johnson, D.F., Ackroff, K., Peters, J., and Collier, G.H. (1986). Changes in rats' meal patterns as a function of the caloric density of the diet. Physiol. Behav. *36*, 929–936.

Kokare, D.M., Patole, A.M., Carta, A., Chopde, C.T., and Subhedar, N.K. (2006). GABA(A) receptors mediate orexin-A induced stimulation of food intake. Neuropharmacology *50*, 16–24.

Konadhode, R.R., Pelluru, D., Blanco-Centurion, C., Zayachkivsky, A., Liu, M., Uhde, T., Glen, W.B., Jr., van den Pol, A.N., Mulholland, P.J., and Shiromani, P.J. (2013). Optogenetic stimulation of MCH neurons increases sleep. J. Neurosci. *33*, 10257–10263.

Kotz, C.M., Wang, C., Teske, J.A., Thorpe, A.J., Novak, C.M., Kiwaki, K., and Levine, J.A. (2006). Orexin A mediation of time spent moving in rats: neural mechanisms. Neuroscience *142*, 29–36.

Kowalski, T.J., Farley, C., Cohen-Williams, M.E., Varty, G., and Spar, B.D. (2004). Melanin-concentrating hormone-1 receptor antagonism decreases feeding by reducing meal size. Eur. J. Pharmacol. *497*, 41–47.

Kremer, E.J., Boutin, S., Chillon, M., and Danos, O. (2000). Canine adenovirus vectors: an alternative for adenovirus-mediated gene transfer. J. Virol. *74*, 505–512.

Lembo, P.M., Grazzini, E., Cao, J., Hubatsch, D.A., Pelletier, M., Hoffert, C., St-Onge, S., Pou, C., Labrecque, J., Groblewski, T., et al. (1999). The receptor for the orexigenic peptide melanin-concentrating hormone is a G-protein-coupled receptor. Nat. Cell Biol. *1*, 267–271.

Ludwig, D.S., Tritos, N.A., Mastaitis, J.W., Kulkarni, R., Kokkotou, E., Elmquist, J., Lowell, B., Flier, J.S., and Maratos-Flier, E. (2001). Melanin-concentrating hormone overexpression in transgenic mice leads to obesity and insulin resistance. J. Clin. Invest. *107*, 379–386.

MacLaren, D.A., Browne, R.W., Shaw, J.K., Krishnan Radhakrishnan, S., Khare, P., Espana, R.A., and Clark, S.D. (2016). Clozapine N-oxide administration produces behavioral effects in Long-Evans rats: implications for designing DREADD experiments. eNeuro *3*.

MacMillan, S.J., Mark, M.A., and Duggan, A.W. (1998). The release of beta-endorphin and the neuropeptide-receptor mismatch in the brain. Brain Res. *794*, 127–136.

Marsh, D.J., Weingarth, D.T., Novi, D.E., Chen, H.Y., Trumbauer, M.E., Chen, A.S., Guan, X.M., Jiang, M.M., Feng, Y., Camacho, R.E., et al. (2002). Melanin-concentrating hormone 1 receptor-deficient mice are lean, hyperactive, and hyperphagic and have altered metabolism. Proc. Natl. Acad. Sci. USA *99*, 3240–3245.

Maulon-Feraille, L., Della Zuana, O., Suply, T., Rovere-Jovene, C., Audinot, V., Levens, N., Boutin, J.A., Duhault, J., and Nahon, J.L. (2002). Appetite-boosting property of pro-melanin-concentrating hormone(131-165) (neuropeptide-glutamic acid-isoleucine) is associated with proteolytic resistance. J. Pharmacol. Exp. Ther. *302*, 766–773.

Muraki, K., Nakata, Y., Simonaka, H., Inoue, J., Hirai, Y., and Akiyama, M. (1996). Neutral endopeptidase activity in serum and cerebrospinal fluid. Hiroshima J. Med. Sci. *45*, 109–112.

Paxinos, G., and Watson, C. (2007). The Rat Brain in Stereotaxic Coordinates, Sixth Edition (Academic Press/Elsevier).

Qu, D., Ludwig, D.S., Gammeltoft, S., Piper, M., Pelleymounter, M.A., Cullen, M.J., Mathes, W.F., Przypek, R., Kanarek, R., and Maratos-Flier, E. (1996). A role for melanin-concentrating hormone in the central regulation of feeding behaviour. Nature *380*, 243–247.

Reiber, H. (2003). Proteins in cerebrospinal fluid and blood: barriers, CSF flow rate and source-related dynamics. Restor. Neurol. Neurosci. *21*, 79–96.

Ripley, B., Overeem, S., Fujiki, N., Nevsimalova, S., Uchino, M., Yesavage, J., Di Monte, D., Dohi, K., Melberg, A., Lammers, G.J., et al. (2001). CSF hypocretin/orexin levels in narcolepsy and other neurological conditions. Neurology *57*, 2253–2258.

Ritter, R.C., Slusser, P.G., and Stone, S. (1981). Glucoreceptors controlling feeding and blood glucose: location in the hindbrain. Science *213*, 451–452.

Shearman, L.P., Camacho, R.E., Sloan Stribling, D., Zhou, D., Bednarek, M.A., Hreniuk, D.L., Feighner, S.D., Tan, C.P., Howard, A.D., Van der Ploeg, L.H., et al. (2003). Chronic MCH-1 receptor modulation alters appetite, body weight and adiposity in rats. Eur. J. Pharmacol. *475*, 37–47.

Sheline, Y.I., West, T., Yarasheski, K., Swarm, R., Jasielec, M.S., Fisher, J.R., Ficker, W.D., Yan, P., Xiong, C., Frederiksen, C., et al. (2014). An antidepressant decreases CSF Abeta production in healthy individuals and in transgenic AD mice. Sci. Transl. Med. *6*, 236re234.

Shimada, M., Tritos, N.A., Lowell, B.B., Flier, J.S., and Maratos-Flier, E. (1998). Mice lacking melanin-concentrating hormone are hypophagic and lean. Nature *396*, 670–674.

Skinner, D.C., and Malpaux, B. (1999). High melatonin concentrations in third ventricular cerebrospinal fluid are not due to Galen vein blood recirculating through the choroid plexus. Endocrinology *140*, 4399–4405.

Sterky, F.H., Lee, S., Wibom, R., Olson, L., and Larsson, N.G. (2011). Impaired mitochondrial transport and Parkin-independent degeneration of respiratory chain-deficient dopamine neurons in vivo. Proc. Natl. Acad. Sci. USA *108*, 12937–12942.

Street, J.M., Barran, P.E., Mackay, C.L., Weidt, S., Balmforth, C., Walsh, T.S., Chalmers, R.T., Webb, D.J., and Dear, J.W. (2012). Identification and proteomic profiling of exosomes in human cerebrospinal fluid. J. Transl. Med. *10*, 5.

Swanson, L.W. (2004). Brain Maps III: Structure of the Rat Brain: An Atlas with Printed and Electronic Templates for Data, Models, and Schematics, Third Revised Edition (Academic Press).

Swanson, L.W., Sanchez-Watts, G., and Watts, A.G. (2005). Comparison of melanin-concentrating hormone and hypocretin/orexin mRNA expression patterns in a new parceling scheme of the lateral hypothalamic zone. Neurosci. Lett. *387*, 80–84.

Veening, J.G., and Barendregt, H.P. (2010). The regulation of brain states by neuroactive substances distributed via the cerebrospinal fluid; a review. Cerebrospinal Fluid Res. *7*, 1.

Veening, J.G., de Jong, T., and Barendregt, H.P. (2010). Oxytocin-messages via the cerebrospinal fluid: behavioral effects; a review. Physiol. Behav. *101*, 193–210.

Vigh, B., Manzano e Silva, M.J., Frank, C.L., Vincze, C., Czirok, S.J., Szabo, A., Lukats, A., and Szel, A. (2004). The system of cerebrospinal fluid-contacting neurons. Its supposed role in the nonsynaptic signal transmission of the brain. Histol. Histopathol. *19*, 607–628.

STAR★METHODS

KEY RESOURCES TABLE

REAGENT or RESOURCE	SOURCE	IDENTIFIER
Antibodies		
Rabbit anti-MCH	Phoenix Pharmaceuticals	RRID: AB_10013632
Mouse anti-synaptophysin	Progen	Cat # 61012
Rabbit anti-RFP	Rockland Inc.	RRID: AB_2209751
Chicken anti-vimentin	Abcam	RRID: AB_778824
Rabbit anti-orexin	Phoenix Pharmaceuticals	RRID: AB_2315019
Mouse anti-beta subunit cholera toxin	Abcam	RRID: AB_300499
Rabbit anti-laminin	Lifespan Biosciences	RRID: AB_1808356
Donkey anti-rabbit IgG-Cy3	Jackson Immunoresearch	RRID: AB_2307443
Donkey anti-rabbit IgG-AlexaFluor 488	Jackson Immunoresearch	RRID: AB_2340619
Donkey anti-mouse IgG-Cy3	Jackson Immunoresearch	RRID: AB_2315777
Donkey anti-mouse IgG-AlexaFluor 488	Jackson Immunoresearch	RRID: AB_2341099
Donkey anti-chicken IgG-AMCA	Jackson Immunoresearch	RRID: AB_2340361
Donkey anti-rabbit IgG- biotin	Jackson Immunoresearch	RRID: AB_2340593
Rabbit anti-PHAL	Vector Laboratories	RRID: AB_2313686
Bacterial and Virus Strains		
AAV2-MCHp-DIO-hM3D(Gq)-mCherry-WPRE	Vector Biolabs (this paper)	(custom)
AAV2-MCHp-hM3D(Gq)-mCherry-WPRE	Vector Biolabs (this paper)	(custom)
CAV2-CRE	Gift from Martin Darvas, PhD	N/A
Chemicals, Peptides, and Recombinant Proteins		
Clozapine N oxide	Generously provided by NIMH	N/A
DMSO	MP Biomedicals, LLC	Cat #: 196055
Protease inhibitor cocktail	Sigma	Cat #: P8340-5ML
aCSF	Harvard Apparatus	Cat #: 59-7316
Melanin concentrating hormone	Bachem	Cat #: H-2218.1000
Donkey serum	Jackson Immunoresearch	Cat #: 017-000-121
Triton-X 100	Sigma	Cat #: X100-500ML
Glycerol	EMD Millipore	Cat #: GX0185-5
Ketaset (Ketamine), 100mg/mL	Henry Schein Animal Health	Cat #: 010177
Anased (Xylazine) Injection, 100mg/mL	Henry Schein Animal Health	Cat #: 033198
Aceproject (Acepromazine) Injection, 10mg/mL	Henry Schein Animal Health	Cat #: 003845
Paraformaldehyde	Alfa Aesar	Cat # A11313
Sodium hydroxide	EMD Millipore	Cat #: SX0590-1
Sodium tetraborate	Alfa Aesar	Cat #: 40114
EDTA Tetrasodium	EMD Millipore	Cat #: EX0550-5
Trizma hydrochloride	Sigma Aldrich	Cat #: T3252-250G
Proteinase K	Sigma Aldrich	Cat #: P2308-100MG
Triethanolamine	Sigma Aldrich	Cat #: T58300-1KG
Acetic anhydride	EMD Millipore	Cat #: AX0080-6
Citric acid trisodium	VWR	Cat #: 0101-500G
ProLong Gold Antifade mounting medium	Cell Signaling	Cat #: 9071S
CTB Alexa Fluor 594	ThermoFisher Scientific	Cat #: C22842
Streptavidin – Alexa Fluor 488	Vector Laboratories	Cat #: SA-5488
MCH Antagonist H6408	Bachem	Cat #: H-6408

(*Continued on next page*)

Continued

REAGENT or RESOURCE	SOURCE	IDENTIFIER
Muscimol	Enzo Life Sciences	Cat #: ALX-550-127-M005
(+/-) Baclofen	Sigma Aldrich	Cat #: B5399
Critical Commercial Assays		
MCH EIA Kit	Phoenix Pharmaceuticals	Cat #: FEK-070-47
vGLUT1 probe	Advanced Cell Diagnostics	Cat #: 317001-C2
vGLUT2 probe	Advanced Cell Diagnostics	Cat #: 317011-C2
vGLUT3 probe	Advanced Cell Diagnostics	Cat #: 476711-C2
RNAscope Fluorescent Multiplex Reagent Kit	Advanced Cell Diagnostics	Cat #: 320851
RNAscope Wash Buffer	Advanced Cell Diagnostics	Cat #: 320058

CONTACT FOR REAGENT AND RESOURCE SHARING

Further information and requests for resources and reagents should be directed to and will be fulfilled by the Lead Contact, Scott Kanoski (kanoski@usc.edu).

EXPERIMENTAL MODEL AND SUBJECT DETAILS

Animals

Male Sprague Dawley rats (Envigo, Indianapolis, IN, USA) weighing 300–400 g and between ages of postnatal day 80–90 were individually housed in wire-hanging cages in a climate controlled (22°C–24°C) environment with a 12 hr: 12hr light/dark cycle. Animals were maintained on a diet of *ad libitum* access to standard rat chow (LabDiet 5001, LabDiet, St. Louis, MO), except where noted. Experiments were performed in accordance with NIH Guidelines for the Care and Use of Laboratory Animals, and all procedures were approved by the local committee of the Institute of Animal Care and Use (University of Southern California).

METHOD DETAILS

Immunofluorescence

Rats were anesthetized and sedated with a ketamine (90 mg/kg)/xylazine (2.8 mg/kg)/acepromazine (0.72 mg/kg) cocktail, then transcardially perfused with 0.9% sterile saline (pH 7.4) followed by 4% paraformaldehyde in 0.1M borate buffer (pH 9.5). Brain dissection, tissue handling, and general immunofluorescence labeling procedures were performed as previously reported (Hsu et al., 2015b). The following antibody dilutions were used: rabbit anti-MCH (1:1000; Phoenix Pharmaceuticals, Burlingame, CA, USA), mouse anti-synaptophysin (1:1000; Progen, Heidelberg, Germany), rabbit anti-RFP (1:2000, Rockland Inc., Limerick, PA, USA), chicken anti-vimentin (1:10,000, Abcam, Cambridge, MA, USA), rabbit anti-orexin A (1:5,000; Phoenix Pharmaceuticals, Burlingame, CA, USA), mouse anti-cholera toxin subunit B (1:500; Abcam, Cambridge, MA, USA), rabbit anti-laminin (1:10,000 Lifespan Biosciences, Seattle, WA, USA). Antibodies were prepared in 0.02 M KPBS solution containing 0.2% BSA and 0.3% Triton X-100 at 4°C overnight. After thorough washing with 0.02M KPBS, sections were incubated with secondary antibody. All secondary antibodies were obtained from Jackson Immunoresearch and used at 1:500 dilution at 4°C, with overnight incubations (Jackson Immunoresearch; West Grove, PA, USA). Sections were mounted and coverslipped using 50% glycerol in 0.02 M KPBS and the edges were sealed with clear nail polish. Photomicrographs were acquired using either a Nikon 80i (Nikon DS-QI1,1280X1024 resolution, 1.45 megapixel) under epifluorescence illumination, or as optical slices using a Zeiss LSM 700 UGRB Confocal System (controlled by Zeiss Zen software).

Fluorescence In Situ Hybridization

Rats were anesthetized and sedated with a ketamine (90 mg/kg)/xylazine (2.8 mg/kg)/acepromazine (0.72 mg/kg) cocktail, then transcardially perfused with 0.9% sterile saline (pH 7.4) followed by 4% paraformaldehyde in 0.1 M borate buffer (pH 9.5). Brains were coronally sectioned to 20 μm on a sliding microtome into 0.02 M KPBS solution. After immunofluorescence staining (see above), sections were mounted onto subbed slides. Slides were placed into a vacuum chamber overnight (~16 hr) to desiccate.

Sections were postfixed in 4% paraformaldehyde in 0.1 M borate buffer (pH 7.4) for 1.75 hr followed by 5 washes in KPBS for 5 min each. Sections were then pretreated by incubating them at 37°C in pretreatment buffer (100 mM Tris buffer and 50mM EDTA in distilled deionized water, pH 8) with 0.001% Proteinase K (Sigma P2308) for 30 min, followed by a 3-min wash in incubation buffer alone and a 3-min rinse in 100 mM Triethanolamine in water (pH 8). Sections were then incubated with 0.25% acetic anhydride in 100 mM triethanolamine for 10 min at room temperature followed by 2 x 2 min washes in saline-sodium citrate buffer (1% citric acid trisodium/2% sodium chloride in water [pH 7.0]). Slides were dehydrated in increasing concentrations of ethanol solution (50%, 70%, 95%, 100%, 100%) for 3 min each and air-dried prior to hybridization.

For hybridization, a hydrophobic barrier was drawn around each section and 3–4 drops of either vGlut1 (317001), vGlut2 (317011), and vGlut3 (476711) probe (Advanced Cell Diagnostics) was placed on each tissue section. Slides were incubated with the probe at 40°C for 3 hr in a HybEz oven (Advanced Cell Diagnostics). Following a 2 -min wash with wash buffer (RNAscope, Advanced Cell Diagnostics 320058) reagents from RNAscope Fluorescent Multiplex Detection Reagent Kit (Advanced Cell Diagnostics, 320851) were applied in order to amplify the probe signal, with AMP1 applied for 45 min, AMP2 for 30 min, AMP 3 for 45 min, and AMP 4 for 30 min. Incubation steps occurred at 40°C, and a 2-min wash followed each amplification step. Slides were coverslipped with ProLong Gold Antifade mounting medium (Cell Signaling, 9071S). Photomicrographs were acquired using a Nikon 80i (Nikon DS-QI1, 1280 × 1024 resolution, 1.45 megapixel) under epifluorescent illumination, or as optical slices using a Zeiss LSM 700 UGRB Confocal System (controlled by Zeiss Zen software).

Cholera Toxin Subunit B (CTB) Injections

Rats were anesthetized and sedated with a ketamine (90 mg/kg)/xylazine (2.8 mg/kg)/acepromazine (0.72 mg/kg) cocktail, and 1 μL injections of 0.5% CTB-Alexa Fluor 594 (ThermoFisher Scientific, Waltham, MA, USA) dissolved in 0.1 M phosphate buffered saline, pH 7.4 were delivered stereotaxically via a Hamilton syringe attached to a PE 20 catheter and injector. Injections were delivered over 30 seconds and injectors remained in the tissue for 2 min post-injection. Injection coordinates for the lateral ventricle were 0.9 mm caudal to bregma, 1.8 mm lateral to the midline (at bregma), and 4.6 mm ventral to the skull at the injection site. Post-operatively, the animals were sutured and analgesic was administered daily for 3 days. Ten days after the tracer injections, animals were transcardially perfused and immunofluorescent staining was performed for either orexin or MCH, as described above. Quantification of MCH, CTB, and CTB positive MCH neurons was performed by manually counting following previously described approaches (Hahn, 2010).

Fast Blue Injections

Rats were anesthetized and sedated with a ketamine (90 mg/kg)/xylazine (2.8 mg/kg)/acepromazine (0.72 mg/kg) cocktail. Animals were shaved and an incision was made in the next to locate the left jugular vein. A 27.5 gauge syringe was inserted and jugular injections of 6 mg/kg body weight Fast Blue (FB) were delivered. Forty-eight hours later, under deep ketamine anesthesia, animals were sacrificed via transcardial perfusion (0.9% saline, followed by 4% paraformaldehyde pH 9.5). Ten days prior to sacrifice, and 8 days prior to FB injections, the animals were injected with CTB in the lateral ventricle, as described. Immunofluorescence labeling was performed for MCH, and quantification of CTB, MCH, and FB labeled neurons in the lateral hypothalamic zone and zona incerta was performed based on one of five series from 3 animals.

Virus Production

For AAVs [AAV2-MCHp-hM3D(Gq)-mCherry-WPRE, and AAV2-MCHp-DIO-hM3D(Gq)-mCherry-WPRE] transgenes were packaged into AAV2s (as previously described (Sterky et al., 2011), Vector Biolabs, Malvern, PA, USA) under the control of an MCH promoter (see below) and delivered at a titer of 8.8×10^{12} GC/mL. The hM3D(Gq) plasmid was obtained from Addgene (#44361; Cambridge, MA, USA). CAV2 CRE was generated as described (Kremer et al., 2000) and had a titer of 3×10^{12} viral genomes per milliliter.

MCH (462 bp) promoter region (Konadhode et al., 2013): TCTAGAGATAACTTCTATTTAATAAGGATTAAAAGGGCATAAAGCTTT TATCCTTATTATCCATGAATTAAATAACACGTCTTAATATCTTAATCGGAAAGTACATAGAAGGTAACTGTAATATTGGGAGAGCCTG GTGTCCTATGGTCTTCCTTAATAACATCCCACTTTCAAGAGGCTATAATCTACTCACAGAAAGCCTTCTCTCAAAGACCTTAATCAG ATTCTGGGAAAATTCACACACGAAATAAACAACAGGCCACTAAATCCAAAACAATGCAAGCATTAGCAGCTTTACAAAGGCGAGGC TCTACGGGGTGATTCATTTCTAAAAAGAAAAGATAAGGCCTTCAAGTGTTTTCTATTCAGGCACAAAGTATATAAAGGTAGGAATCA TTCAGTCGCCAGCAGAGTGTGGCATTCTCCCCACATTCTCTTCGGCTTTACGGAGCAGCAAACAGG.

Virus Injections

Rats were anesthetized and sedated with a ketamine (90 mg/kg)/xylazine (2.8 mg/kg)/acepromazine (0.72 mg/kg) cocktail. Stereotaxic injections of MCH AAV2-rMCHp-hM3D(Gq)-mCherry were delivered using a microinfusion pump (Harvard Apparatus) connected to a 33-gauge microsyringe injector attached to a PE20 catheter and Hamilton syringe. Flow rate was calibrated and set to 5μL/min; injection volume was 300 nL/site. Injectors were left in place for 2 min post-injection. Bilateral injections of the AAV2 virus were given to the following coordinates (Paxinos and Watson, 2007): injection 1, −2.6 mm AP, ± 1.8 mm ML, −8.0 DV; injection 2, −2.6 mm AP, ± 1.0 mm ML, −8.0 DV; injection 3, −2.9 mm AP, ± 1.1 mm ML, −8.8 DV; injection 4, −2.9 mm AP, ± 1.6 mm ML, −8.8 DV (from the skull surface at bregma). Animals were allowed to incubate with the virus for 21 days prior to experimentation. Successful virally mediated transduction of the DREADDs receptor was confirmed post-mortem in all animals (n = 8) via immunohistochemical staining using an RFP primary antibody to enhance the mCherry signal followed by manual quantification under epifluorescence illumination using a Nikon 80i (Nikon DS-QI1,1280X1024 resolution, 1.45 megapixel).

The cre-dependent AAV2-DIO-rMCHp-hM3D(Gq)-mCherry was injected in four bilateral (8 total) injections as described in the methods above. Prior to injections with the MCH AAV2-DIO-rMCHp-hM3D(Gq)-mCherry, a unilateral injection of the canine adenovirus 2 Cre (CAV2 CRE; 1.5 μL) was stereotaxically injected into the lateral ventricle using the following coordinates (Paxinos and Watson, 2007): −0.9 mm AP, 1.8 mm ML, −4.6 mm DV (from the skull surface at the injection site). Animals were allowed to incubate with the virus for 21 days prior to experimentation. Successful virally mediated transduction of the DREADDs receptor was confirmed post-mortem in all animals (n = 7) via immunohistochemical staining using an RFP primary antibody to enhance the mCherry signal

followed by manual quantification under epifluorescence illumination using a Nikon 80i (Nikon DS-QI1,1280 × 1024 resolution, 1.45 megapixel).

In a separate cohort of animals, the cre-dependent AAV2-DIO-rMCHp-hM3D(Gq)-mCherry was injected in four bilateral (8 total) injections as described in the methods above. Prior to injections with the MCH AAV2-DIO-rMCHp-hM3D(Gq)-mCherry, bilateral injections of the canine adenovirus 2 Cre (CAV2 CRE; 200 nL/side) were stereotaxically injected into the nucleus accumbens shell using the following coordinates (Paxinos and Watson, 2007): 1.1 mm AP, ±0.8 mm ML, −7.5 mm DV (from the skull surface at bregma). Animals were allowed to incubate with the virus for 21 days prior to experimentation and successful transduction of the DREADDs was confirmed as described above.

Characterization of DREADDs Expression

In all cases where DREADDs transduction occurred, the spread of DREADDs expression was quantified in 1 out of 5 series of brain tissue sections from perfused brains cut at 30 μm on a microtome with a frozen stage. Sections from Swanson Brain Atlas level 27-32 (Swanson, 2004), which encompasses all MCH containing neurons, were selected using anatomical landmarks and immunofluorescence staining for red fluorescent protein (RFP) was conducted to amplify the mCherry signal (as described above). Cell counts were performed by 2 researchers under epifluorescence illumination using a Nikon 80i (Nikon DS-QI1,1280 × 1024 resolution, 1.45 megapixel) and the average of the 2 counts was taken. Researchers who performed the counting were kept consistent between cohorts and blind to experimental assignments. In cases where the anatomical location of the cells was identified, experimenters utilized anatomical landmarks from the Swanson Brain Atlas (Swanson, 2004) to characterize regions of cell localization.

I.c.v. Cannula Implantation

Unilateral guide cannulae (26-gauge, Plastics One) were surgically implanted targeting the lateral ventricle as previously described (Hsu et al., 2015b) using the following coordinates (Paxinos and Watson, 2007): −0.9 mm AP, 1.8 mm ML, −2.6 mm DV. Placement for the lateral ventricle cannula was verified by elevation of cytoglucopenia resulting from an injection of 210 μg (2 μL) of 5-thio-D-glucose (5tg) (Ritter et al., 1981) using an injector that extended 2 mm beyond the end of the guide cannula. A post-injection elevation of at least 100% of baseline glycemia as required for subject inclusion. Animals that did not pass the 5tg test were retested with an injector that extended 2.5 mm beyond the end of the guide cannula, and upon passing 5tg were subsequently injected using a 2.5 mm injector instead of a 2 mm injector for the remainder of the study.

Effect of Activation of MCH Neurons on Food Intake

All injections were delivered through a 33-gauge microsyringe injector attached to a PE20 catheter and Hamilton syringe. The microsyringe injector extended either 2 or 2.5 mm beyond the end of the guide cannula targeting the lateral ventricle. For testing the effects of activating MCH neurons in rats with the MCH AAV2-rMCHp-hM3D(Gq)-mCherry on feeding, injections of artificial cerebrospinal fluid (Harvard Apparatus, Holliston, MA, USA; aCSF; 1μL), the MCH antagonist H6408 (Bachem, Torrance, CA, USA; 10 μg in 1 μL aCSF), Clozapine-N-Oxide (National Institute of Mental Health; 18 mmoles in 2 μL), or 33% DMSO in aCSF (daCSF; 2 μL) were given in a mixed design, with aCSF and H6408 as a between subjects variable and CNO and daCSF as a within subjects variable (n = 15). Food was removed one hour prior to injections, which were given 30 min prior to the onset of the dark cycle. Food hoppers were weighed and placed in cages post injections and food intake was measured by subtracting the hopper weight at 2 hr from the time the animal received the food from the initial hopper weight. For each animal, spillage was collected from papers that were placed beneath the wire hanging cages and subtracted from the differences of hopper weight to get a measure of total intake.

Activation of Ventricular Projecting MCH Neurons

Food was removed at the beginning of the light cycle. Injections of Clozapine-N-Oxide (National Institute of Mental Health; 18 mmoles in 2 μL), or 33% DMSO in aCSF (daCSF; 2 μL) were administered 1.5 hr into the light cycle, and food intake was monitored. Food hoppers were weighed and placed in cages post injections and food intake was measured by subtracting the hopper weight at 2 and 4 hr from the time the animal received the food from the initial hopper weight. For each animal, spillage was collected from papers that were placed beneath the wire hanging cages and subtracted from the differences of hopper weight to get a measure of total intake for each time point. A within subject's design was used, where animals were injected with either CNO or vehicle in a counterbalanced fashion for a total of 2 treatments with 72 hr between treatments (n = 7). This experiment was replicated once with similar results and was also replicated using a different retrograde virus (AAV6-CRE) with similar results.

Activation of ACB Projecting MCH Neurons

Food was removed at the beginning of the light cycle. Injections of Clozapine-N-Oxide (National Institute of Mental Health; 18 mmoles in 2 μL), or 33% DMSO in aCSF (daCSF; 2 μL) were administered 1.5 hr into the light cycle, and food intake was monitored. Food hoppers were weighed and placed in cages post injections and food intake was measured by subtracting the hopper weight at 2 and 4 hr from the time the animal received the food from the initial hopper weight. For each animal, spillage was collected from papers that were placed beneath the wire hanging cages and subtracted from the differences of hopper weight to get a measure of total intake for each time point. A within subject design was used, where animals were injected with either CNO or vehicle in a counterbalanced fashion for a total of 2 treatments with 72 hr between treatments (n = 11).

Brain Slice Preparation

Rats (n = 7) were anesthetized by inhalation of isoflurane gas (2%-4%) and decapitated by guillotine. The brain was removed and placed for 1 min in cold (0°C–4°C) artificial cerebrospinal fluid (aCSF) composed of the following (in mM): NaCl 125, KCl 3, KH_2PO_4 1.2, $MgSO_4$ 1.2, $NaHCO_3$ 25, dextrose 10, $CaCl_2$ 2, and bubbled with 95% O_2/5% CO_2 (pH 7.4, 306–310 mOsM adjusted with sucrose). A tissue block was mounted in a vibrating microtome (Leica VT-1000S). Coronal slices (300 μm thick) were cut with a sapphire knife (Delaware Diamond Knives, Wilmington, DE), submerged in a microscope chamber, and perfused with oxygenated aCSF at a rate of 2 mL/min.

Electrophysiology

Lateral hypothalamic area neurons were visually selected for electrophysiological patch clamp recordings using a fluorescence microscope (Olympus BX51WI). Patch electrodes were guided to neurons using differential interference contrast (DIC) optics illuminated with infrared light. Current-clamp recordings were made with a MultiClamp 700B amplifier, Digidata 1440A digitizer, and pClamp10.2 software (all from Molecular Devices, Sunnyvale, CA). Data were filtered at 10 kHz, and stored on a personal computer for offline analysis. For recordings, patch pipettes were pulled using a pipette puller (P-2000, Sutter Instruments, Novato, CA). The pipette resistance was 3.0–4.0 MΩ when filled with internal solution (in mM: NaCl 10, K-'gluconate 130, EGTA 11, $CaCl_2$ 1, $MgCl_2$ 2, HEPES 10, Na-ATP 2, Na-GTP 0.2, pH 7.3, 297–300 mOsM). After formation of a stable giga-ohm seal (>2 GΩ), the whole-cell configuration was established. Only neurons with holding currents not exceeding −100pA at V_H = −60 mV for the 15 min control period (membrane resistance >250 MΩ) were studied further (n = 8). Series resistance (R_a) was measured at the beginning and end of recordings and neurons were not included in additional analysis if it exceeded 20 MΩ, or drifted >25%. R_a did not differ between control (aCSF) and drug treatment. aCSF was heated to 32°C ± 0.5°C using a pre-heater, a temperature sensor positioned on the wall of the recording chamber next to the slice, and a temperature controller (Cell Micro Controls, Norfolk, VA). The extracellular solution was identical to oxygenated aCSF that was used for the brain tissue preparation.

CSF Extraction and MCH Enzyme Immuno Assay

Rats were deeply anesthetized using a cocktail of ketamine 90 mg/kg, xylazine 2.8 mg/kg, and acepromazine 0.72 mg/kg by intramuscular injection. Shaved and prepped rats were then placed into stereotaxic ear bars, with the head angled downward. An incision was made along the back of the neck and the muscles were blunt dissected with a tissue retractor. A spatula was used to clear the spongy dura that is caudally adjacent to the base of the skull; this is the point of insertion into the medullary cisterna. A sterile 1 mL syringe with 27-gauge needle was attached to the stereotaxic arm with the open side of the bevel facing the posterior end of the rat. After pulling 1 mL of air, the needle was lowered to below the caudal end of the occipital skull and the dura was punctured slowly, moving the stereotaxic arm up and down (less than 1 mm each direction) to imitate a sawing motion. The needle was lowered another ~2 mm and the syringe plunger pulled back, allowing the clear CSF to flow into the syringe. After extracting ~200 mL of CSF, the needle was raised quickly (to prevent suction of blood while coming out of the cisterna magna) and the CSF dispensed into a microfuge tube and immediately frozen in dry ice and stored at −80°C until time of analysis. Quantification of MCH levels in CSF was performed according to manufacturer's instructions using an EIA kit (Phoenix Pharmaceuticals, Burlingame, CA, USA).

CSF Extraction Following MCH DREADDS Activation

For the effects of activation of MCH DREADDs on MCH levels in CSF, animals were injected with either 33% DMSO in aCSF (daCSF; 2 μL) or Clozapine-N-Oxide (National Institutes of Health; 18 mmoles in 2 μL) 2 hr prior to perfusion and again 15 min prior to perfusion (n = 6 and 7). CSF extractions and perfusions were performed in a counterbalanced manner beginning 2 hr into the light cycle.

Effect of Physiological Parameters on CSF MCH Levels

To determine whether MCH levels in CSF fluctuate based on time of day, CSF was extracted either 1 hr into the dark cycle, or 3 hr into the light cycle (n=8/group). Food was removed 2 hr prior to CSF extraction. To determine whether MCH levels in CSF were altered as a function of prandial state (pre vs post) animals were meal entrained to the first 4 hr of the dark cycle. On the day of extraction, a standardized meal of 5 grams of chow was given at the start of the dark cycle. All animals consumed all of the chow in less than 1 hr, and CSF extractions occurred 1 hr into the dark cycle (n = 8).

To determine whether MCH levels in CSF are elevated prior to feeding when animals are entrained to light cycle feeding, rats were first divided into two groups (light entrained or *ad libitum* fed) matched for body weight. On day zero, a baseline 4-hr cumulative food intake recording was measured during mid-light cycle period (ZT4-ZT8) when light entrained animals would subsequently receive all of their daily chow. The experimental group was then meal entrained for 18 days whereas the control group received *ad libitum* food access. Food intake and spillage were monitored during the 4-hr entrainment period for both the *ad libitum* fed control animals and the light entrained animals. CSF was extracted at ZT4 when food would normally be given to the light entrained animals (n=7/group) with food removed 1 hr prior to extraction from the *ad libitum* fed animals.

To determine whether consumption of a palatable high fat/sucrose diet increases pre-prandial levels of MCH, animals were randomized to receive either chow (controls) or a diet containing 45% kcal from fat (Research Diets, D12451). Animals were maintained on the diet for 5 days, and food intake, spillage, and body weights were recorded. Food was pulled 1 hr prior to CSF extraction, and CSF was extracted at the time of the dark cycle onset (Z12) (n = 6/group).

To determine whether MCH levels in CSF were affected by acute food restriction, animals were either food deprived for 48 hours (48-hr food dep., n = 5) or fed *ad libitum* (n = 6). Animals were divided based on body weight such that each group was of equal body weight at baseline. Food was removed 30 min prior to CSF extraction for the *ad libitum* fed animals. CSF was extracted during the late dark cycle (ZT18).

MCH Dose Response and CSF Extraction

Male Sprague Dawley rats (n=12) were surgically implanted with i.c.v. guide cannula and cannula placement was verified as described above. Animals were handled and habituated to injections prior to testing. On test day, food was removed 1 hr prior to injections, which occurred at ZT5. All injections were delivered through a 33-gauge micro-syringe injector attached to a PE20 catheter and Hamilton syringe. The micro-syringe injector extended either 2 or 2.5 mm beyond the end of the guide cannula targeting the lateral ventricle. Animals were randomized to receive either 0 (aCSF), 0.5 μg, or 1 μg of MCH in 1 μL of aCSF vehicle in a counterbalanced within subject's design. Injections were given during the light cycle such that food was replaced at ZT 6. On each treatment day, food was removed 1 hr prior to injections and replaced immediately following the last injection. Food intake and spillage under the cage was weighed and recorded.

For the CSF extraction following injections with the least effective dose of MCH for hyperphagia, rats (n = 19) were injected with 1 μg of MCH or vehicle and anesthetized beginning either 45 min (n = 4 and 3, respectively) or 1 hr and 45 min (n = 6/group) later. CSF was extracted during the time window of either 60–90 min post MCH/vehicle injection or 120–150 min. Samples were treated with protease inhibitor and frozen and MCH levels were quantified in CSF using a commercial EIA kit as described above.

Co-injections of MCH and GABA-A or GABA-B Agonists

Male Sprague Dawley rats were surgically implanted with i.c.v. guide cannula and cannula placement was verified as described above. Animals were handled and habituated to injections prior to testing. On test day, food was removed 1 hr prior to injections, which occurred at ZT5. All injections were delivered through a 33-gauge microsyringe injector attached to a PE20 catheter and Hamilton syringe. The microsyringe injector extended either 2 or 2.5 mm beyond the end of the guide cannula targeting the lateral ventricle. For the dose response of muscimol, animals were randomized to receive either 0 (aCSF), 25 ng, or 75 ng of muscimol in 1 μL of aCSF vehicle in a counterbalanced within subject's design (n = 12; 3–4 days separating treatments). On each treatment day, food was removed 1 hr prior to injections and replaced immediately following the last injection. Food intake and spillage under the cage was weighed and recorded. As food intake readings were trending towards significance ($p = 0.07$ at 1 hr) at the 25 ng dose, we used a 20 ng dose of muscimol for our co-injection experiment to test whether muscimol (at a dose ineffective for food intake effects alone) would potentiate an orexigenic effect of a sub-effective dose of MCH (0.5 μg). Using a counterbalanced, within-subject's design, animals (n = 12) were randomized to receive either 0 (aCSF) or 0.5 μg of MCH and either 0 (aCSF) or 20 ng of muscimol (four treatments total: aCSF-aCSF, MCH-aCSF, aCSF-muscimol, MCH-muscimol). Injections of MCH were given 1 hr prior to injections of muscimol, beginning at ZT5. Food was replaced after the last muscimol injection and food intake and spillage under the cage were recorded. The same parameters and experimental design were used for MCH and Baclofen co-injection experiments; however, for baclofen experiments a mixed design was used (n = 17 animals total) with MCH vs aCSF (vehicle) as the within-subject's variable and Baclofen vs aCSF (vehicle) as the between-subject's variable. The dose of Baclofen used was 0.1 nmol in 1 μL of aCSF based on (Ebenezer, 1990).

Injections of Neutralizing Antibody in the CSF

Rats were surgically implanted with i.c.v. cannula and cannula placement was verified as described above. On the day of testing, food was removed 1.5 hr prior to injections, which began 30 min prior to the onset of the dark cycle. All injections were delivered through a 33-gauge micro-syringe injector attached to a PE20 catheter and Hamilton syringe. The micro-syringe injector extended either 2 or 2.5 mm beyond the end of the guide cannula targeting the lateral ventricle. Injections of 2 μL of either rabbit anti-MCH (n = 10) or rabbit anti-PHAL (control; n = 9) in a 1:1 dilution of aCSF were delivered to the lateral ventricle. All injections were completed within 30 min and food (standard chow) was returned to the animals at the onset of the dark cycle. Food intake and spillage was recorded as described above. Animals were perfused following the 8-hr food intake reading and brains were dissected out and sectioned as described above.

Immunosequestration of MCH in CSF

Rats were surgically implanted with i.c.v. cannula and cannula placement was verified as described above. On the day of testing, food was removed 30 min prior to injections, which began 2 hr prior to the onset of the dark cycle. All injections were delivered through a 33-gauge micro-syringe injector attached to a PE20 catheter and Hamilton syringe. The micro-syringe injector extended either 2 or 2.5 mm beyond the end of the guide cannula targeting the lateral ventricle. Three injections were given 30 min apart: injection 1, 1:1 mixture of biotinylated donkey anti-rabbit with rabbit anti-laminin, 2 μl injection volume; injection 2, Streptavidin conjugated to Alexa Fluor-488, 1 μl injection volume; and injection 3, 1:1 mixture of biotinylated donkey anti-rabbit premixed with either rabbit anti-MCH (n = 9) or rabbit anti-PHAL (n = 8). Antibody mixtures were prepared in 0.9% saline 24 hr prior to injections and stored at 4°C. Food was replaced following the last injection and food intake was measured as described above.

Comparison of Neuropil Penetrance

Immunofluorescence visualization of the antibody in the tissue was performed using the immunofluorescence staining methods above but omitting the addition of primary antibody. The addition of secondary antibody (Donkey anti-rabbit-Cy3) enabled the detection of rabbit anti-MCH primary antibody in tissue sections from both groups. Tissue sections were stained in the same run to avoid variation in staining quality and allow for equal comparisons. Images were collected using identical microscope and imaging parameters using epifluorescence illumination using a Nikon 80i (Nikon DS-QI1,1280X1024 resolution, 1.45 megapixel).

QUANTIFICATION AND STATISTICAL ANALYSIS

Statistical Analyses

ANOVA analyses were performed using GraphPad Prism 7.0 Software (GraphPad Software Inc.) and t tests were performed using either GraphPad Prism 7.0 Software or Microsoft Excel for Mac (v. 15.26; Microsoft Inc.). To investigate the effects of MCH DREADDs activation on CSF MCH levels, data were analyzed using a Student's two-tailed unpaired t test with Welch's correction for unequal variances. Comparisons of the effects of CNO on food intake in animals with or without prior injections of the MCH receptor 1 antagonist, which were analyzed using a mixed design with H6408 vs vehicle at the between subjects group and CNO vs vehicle as the within subjects group. These data were analyzed using Two-way repeated measures ANOVA with a mixed design and Newman-Keuls post hoc test to adjust for multiple comparisons. Statistica Software (StatSoft, Inc.). For the muscimol dose response experiment, data are analyzed at each time point using a repeated measures one-way ANOVA with Geisser-Greenhouse correction and Tukey's multiple comparisons test. For the muscimol combined with a low dose of MCH experiment, data are analyzed using a repeated measures two-factor ANOVA (Drug 1 x Drug 2) at each time point. For the Baclofen experiment data are analyzed using a mixed design two-factor ANOVA (Drug 1 x Drug 2) at each time point with MCH vs vehicle as the within- subject variable and Baclofen vs vehicle as the between subject variable. For the electrophysiological recordings, data were analyzed using one-way ANOVA with Tukey's post hoc test for multiple comparisons. For all statistical tests, the α level for significance was .05.

DATA AND SOFTWARE AVAILABILITY

Data Resources

All data generated and analyzed for this manuscript are available from the corresponding author (S.E.K.) upon reasonable request.

Cell Metabolism, Volume *28*

Supplemental Information

Control of Feeding Behavior by Cerebral Ventricular Volume Transmission of Melanin-Concentrating Hormone

Emily E. Noble, Joel D. Hahn, Vaibhav R. Konanur, Ted M. Hsu, Stephen J. Page, Alyssa M. Cortella, Clarissa M. Liu, Monica Y. Song, Andrea N. Suarez, Caroline C. Szujewski, Danielle Rider, Jamie E. Clarke, Martin Darvas, Suzanne M. Appleyard, and Scott E. Kanoski

Supplemental figures

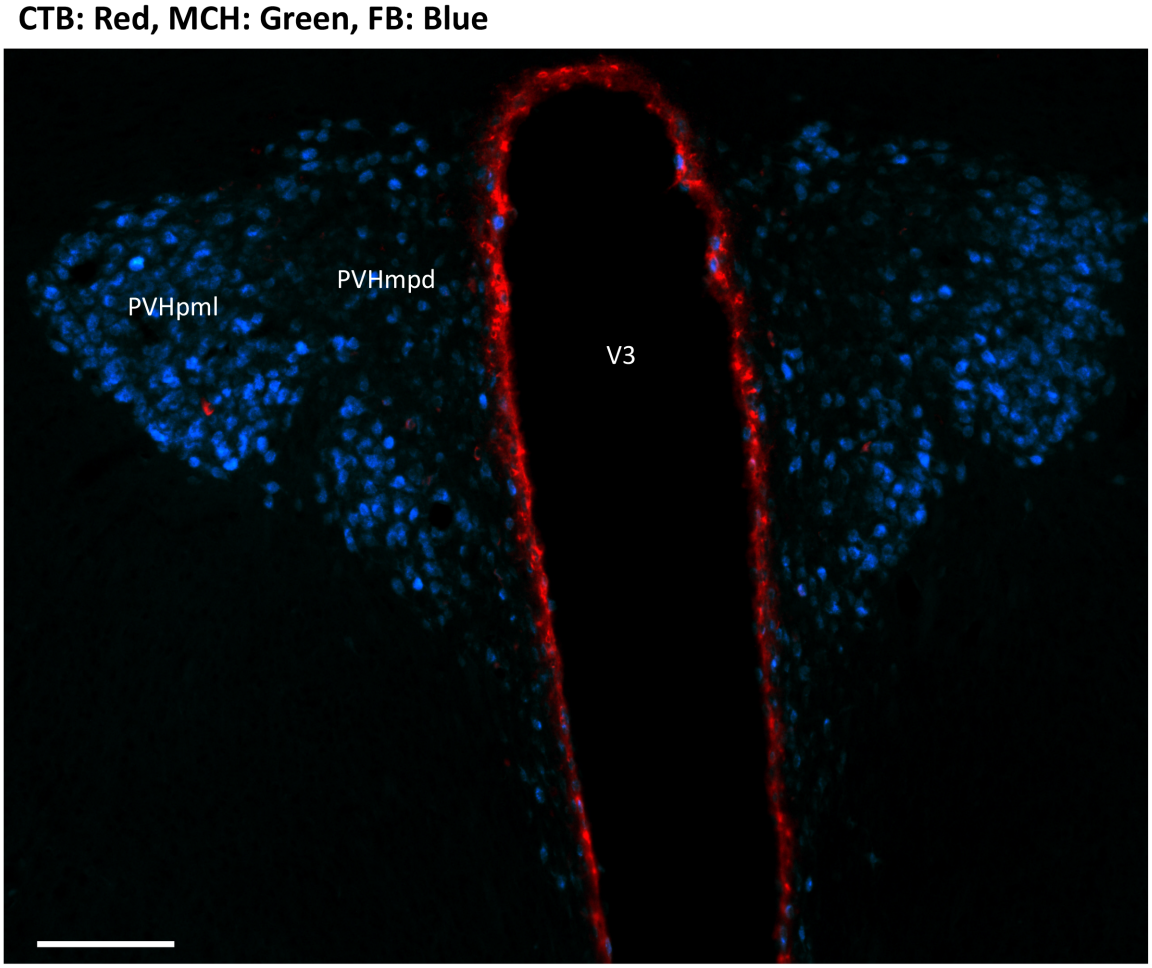

Figure S1 (related to Figures 2C): Neuroendocrine neurons in the hypothalamic paraventricular nucleus (PVH) do not signal through neural-CSF signaling pathways.

A representative image at a mid-rostrocaudal level of the PVH showing cholera toxin subunit B (CTB) retrograde labeling (red) after lateral ventricular CTB injection, and fast blue (FB) retrograde labeling (blue) after intravenous FB

injection. Note that there are few CTB-labeled PVH neurons, and none is positive for FB. Immunofluorescence was also applied for melanin-concentrating hormone (MCH; green), confirming the absence of MCH-expressing somata in the PVH. Abbreviations: PVHpml = paraventricular hypothalamic nucleus, posterior magnocellular part, lateral zone; PVHmpd = paraventricular hypothalamic nucleus, medial parvicellular part, dorsal zone; V3 = third ventricle. Scale bar: 100 μm.

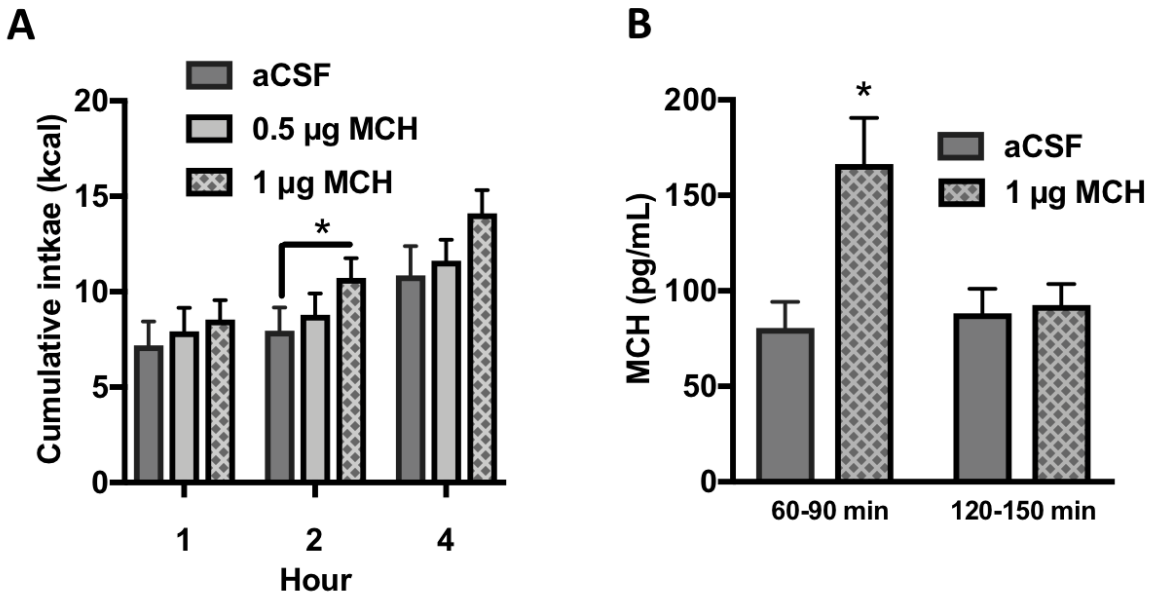

Figure S2 (related to Figures 5E and 6C): ICV injection of the smallest effective dose of MCH for hyperphagia elevates MCH levels by comparable amounts compared to chemogenetic MCH neuron activation.

(A) A dose response experiment for ICV MCH administration effects on feeding revealed that 1 µg was the least effective dose required to elevate chow intake during the light cycle (n=12). (B) MCH levels in the CSF were measured by enzyme immunoassay following injection of the least effective dose MCH for ICV feeding effects (1 µg). CSF MCH levels were elevated at between 60-90 minutes post injection (166.4 ± 24.1 SEM for MCH vs 80.5 ± 13.7 SEM for aCSF; n=3-4/group) and are back to baseline by 120-150 min post injection (n=6/group) ($^{*}P<.05$).

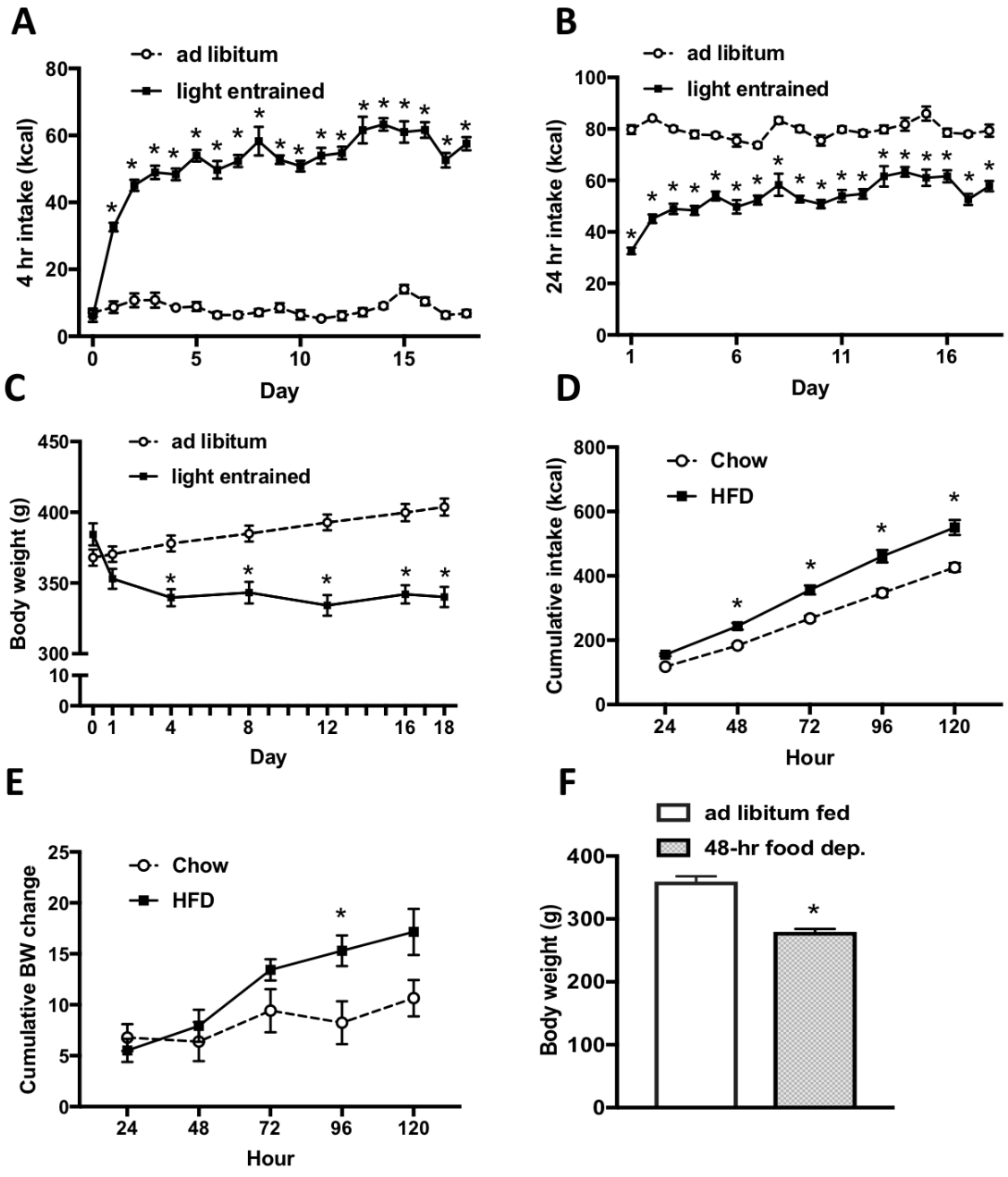

Figure S3 (related to Figure 6E-G): Food intake and/or body weight data for experiments testing endogenous levels of CSF MCH following meal entrainment (A-C), high fat diet maintenance (D,E) and 48 hour food restriction (F).

(A) Food intake data revealed a significant interaction (group x time) for 4 hour chow intake during the meal entrainment period (n=7/group). Food intake was significantly elevated in meal entrained animals during the 4 hour light cycle period compared with ad libitum fed animals. (B) Food intake data revealed a significant interaction (group x time) for 24 hour chow intake. Animals in the meal-entrainment group consumed significantly less chow throughout the study period. (C) Body weights were significantly reduced in the meal entrainment group. (D) Animals fed a high fat diet (HFD) consumed significantly more kcals compared with animals fed chow (n= 6/group). (E) Body weight gain from baseline was significantly elevated in the HFD group compared with chow fed animals by 96 hours of exposure to the diet and at the time of CSF extraction (120 hours). (F) Body weights were significantly reduced following 48 hours of food deprivation compared with ad libitum fed control animals (initial body weights were 337.7 ± 4.3 and 337.4 ± 7.5 for 48 hr food restricted and ad libitum groups, respectively, n=5-6/group) (*$P<.05$).

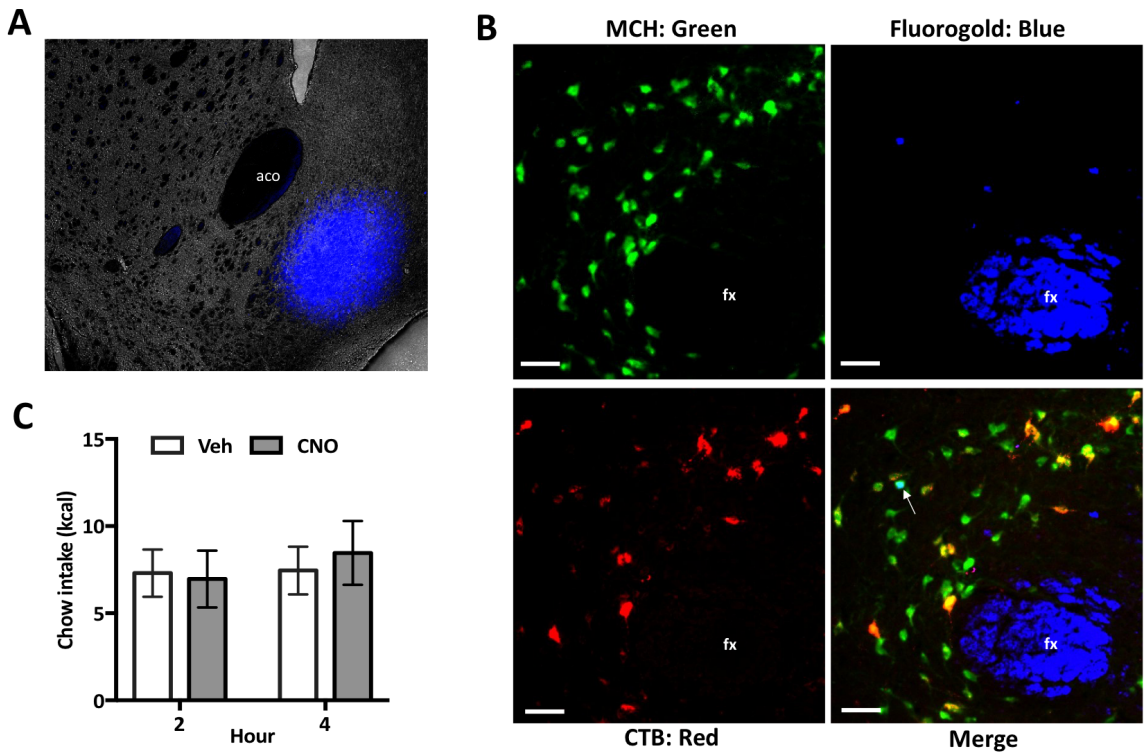

Figure S4 (related to Figure 7A-C): CSF-projecting MCH neurons do not send axon collaterals to the nucleus accumbens shell (ACBsh) – an established site of action for MCH-driven hyperphagia.

(A) A representative image showing an injection site for the retrograde tracer FluoroGold (FG) in the ACBsh. B) A representative image, and very rare example, of a triple-labeled FG (blue, pseudocolored), MCH (green), and CTB (red) labeled neuron in the lateral hypothalamic area. Only 0.08% of CTB and MCH labeled neurons were also FG labeled, indicating a general absence of combined synaptic and CSF-signaling by MCH neurons that target the ACBsh. (C) Activation of MCH neurons that project to the ACBsh by lateral ventricular injections of CNO (using the dual virus approach described in Figure 7, with CAV2-CRE targeting

the ACBsh) had no effect on food intake (n=11). Abbreviations: aco = anterior commissure; fx = fornix. Scale bar = 50 μm.

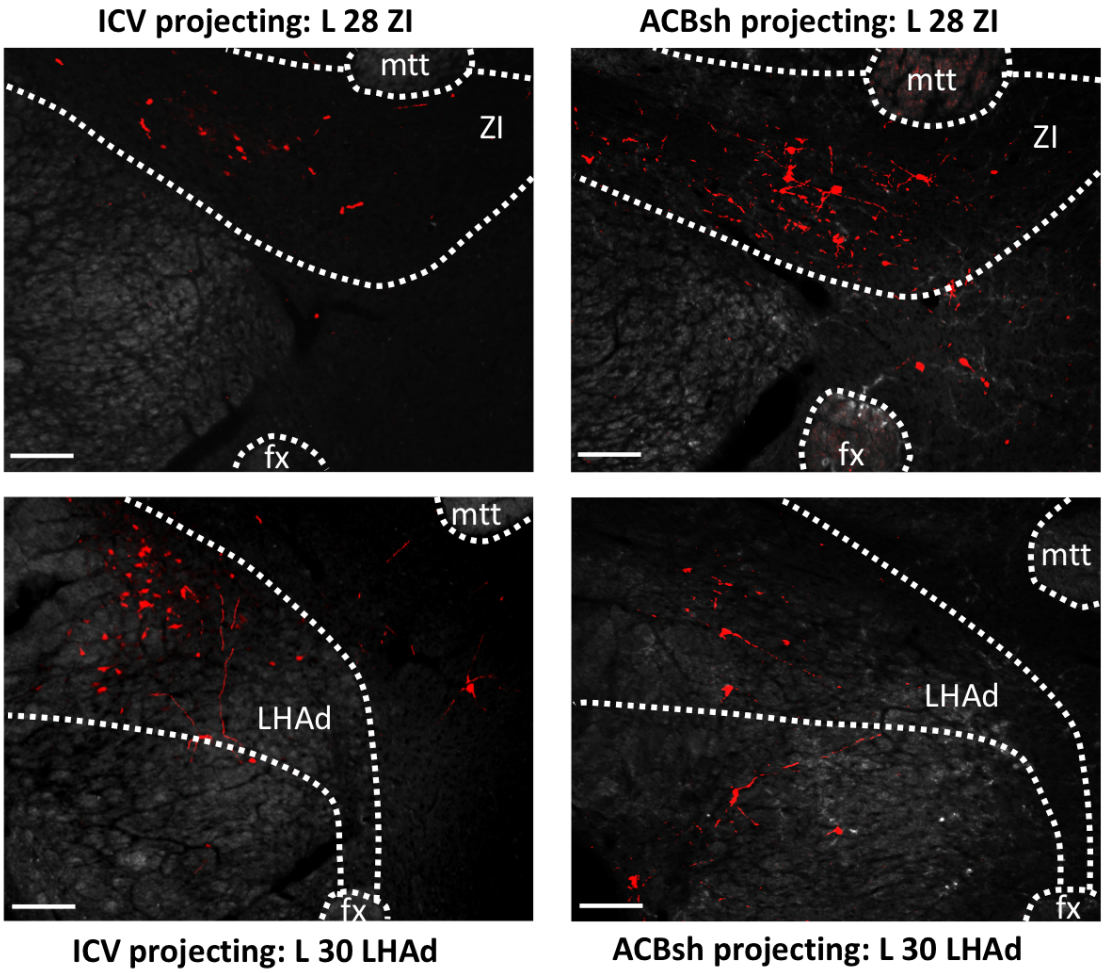

Figure S5 (related to Figure 7A-C and Figure S4): Comparison of the distribution of ACBsh- and ventricular- projecting MCH neurons that were transduced with DREADDs.

Representative images showing RFP immunofluorescence amplified mCherry positive cells in brain sections from animals injected using a dual virus approach where CAV2-CRE was either injected intracerebroventricularly (ICV) or into the nucleus accumbens shell (ACBsh). Atlas levels (L) are based on the Swanson Rat Brain Atlas (Swanson, 2004). Abbreviations: mtt = mammillothalamic tract; fx =

fornix; LHAd = lateral hypothalamic area, dorsal; ZI = zona incerta. Scale bars = 100 μm.

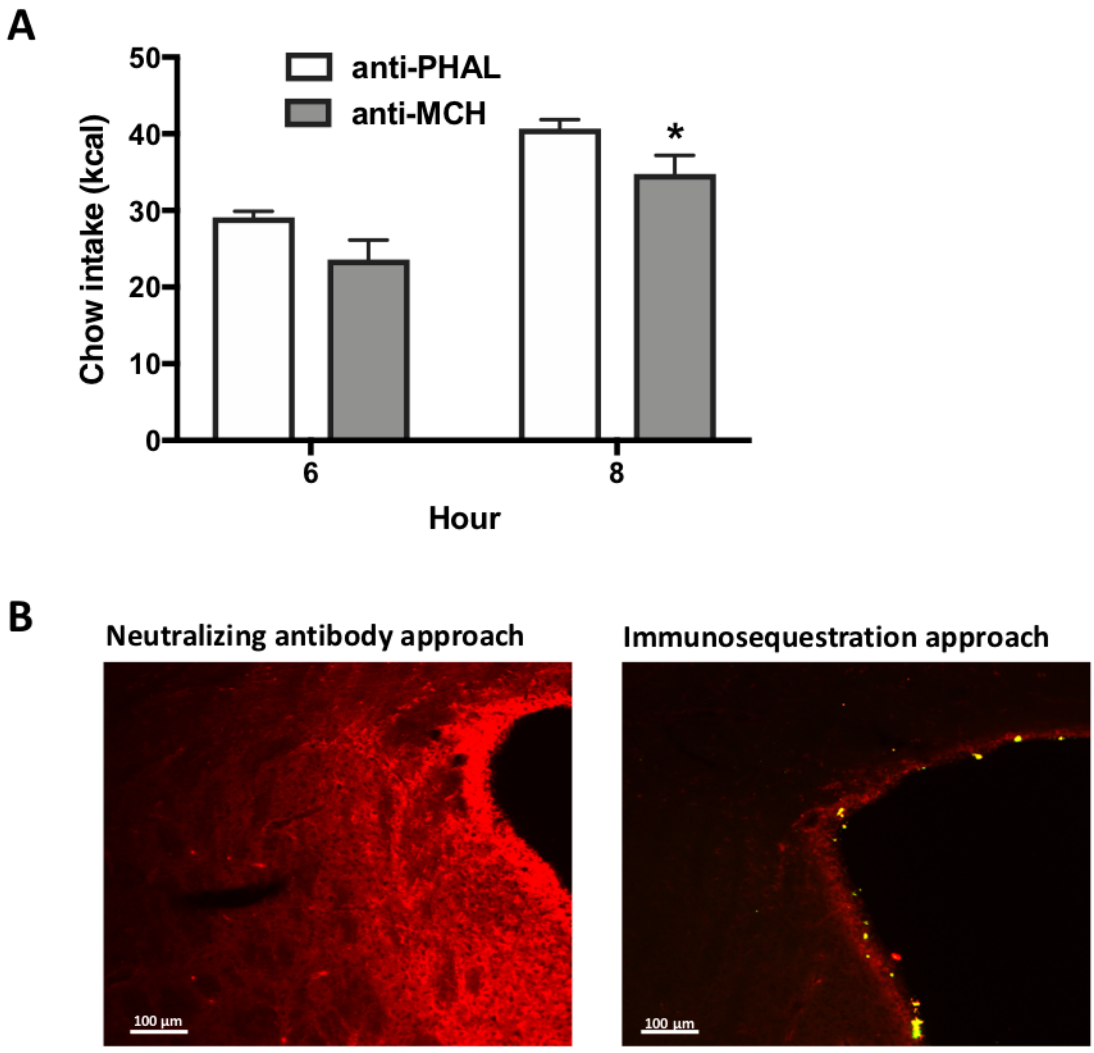

Figure S6 (related to Figure 7D-G): Injections of a neutralizing MCH antibody significantly reduce food intake.

(A) Cumulative intake of chow in animals given injections of either a neutralizing antibody against MCH or an antibody against a non-endogenous control molecule (PHAL) were given just prior to the onset of the dark cycle. Food intake

was significantly reduced 8 hours into the dark cycle in animals injected with the MCH neutralizing antibody (n=9-10). (B) Representative immunofluorescence images from the neutralizing antibody (left) and immunosequesteration approaches (right, from Figure 7). Brain tissue sections were treated with Cy3 secondary antibody against the MCH primary antibody (red). With the Neutralizing antibody approach, it appears that MCH diffused into the neuropil, as evidenced by the red haze surrounding the ventricle at the injection site. Conversely there appears to be minimal antibody diffusion in the neuropil following the immunosequesteration approach. Scale bars = 100 μm (*P<.05).